JOURNAL OF QUATERNARY SCIENCE (2026) 1–16 ISSN 0267-8179. DOI: 10.1002/jqs.70069

JQS Journal of Quaternary Science QRA Quaternary Research Association

Insights into Red Deer Ecology during the Late Epigravettian: New isotopic evidence from Riparo Tagliente (Italian Prealps)

MAHYM AMANOVA,[1*] DOROTHÉE G. DRUCKER[2*] and FEDERICA FONTANA[3]

[1]Instituto Politécnico de Tomar, Tomar, Portugal

[2]Department of Geoscience, Senckenberg Centre for Human Evolution and Palaeoenvironment, University of Tübingen, HUMAN ORIGINS—Cluster of Excellence for Integrative Human Origins Studies (EXC 3101), Tübingen, Germany

[3]Department of Humanities, Section of Prehistoric and Anthropological Sciences, University of Ferrara, Ferrara, Italy

*Present Address: Instituto Terra e Memória – Centro de Geociências, Mação, Portugal

Received 2 July 2025; Revised 26 February 2026; Accepted 16 March 2026

ABSTRACT: The transition from the Last Glacial Maximum to the Late Glacial marked a shift from the cold conditions of Greenland Stadial-2 (GS-2) to the warmer phases of Greenland Interstadial-1 (GI-1), enabling the reoccupation of Alpine regions by Late Palaeolithic hunter-gatherers. Riparo Tagliente, a rockshelter in northeastern Italy, preserves the most extensive Late Glacial stratigraphy in the southeastern Alps and provides key evidence for early human re-settlement by Late Epigravettian groups. To investigate environmental conditions and resource stability, we analyzed stable carbon and oxygen isotopes ($\delta^{13}C_{carb}$, $\delta^{18}O_{carb}$) in enamel carbonate from red deer (*Cervus elaphus*) second and third molars across stratigraphic units 13 to 5, spanning GS-2.1a to GI-1. Tooth $\delta^{13}C$ values reflect a diet based on C3 plants within relatively open woodland environments, showing limited change across climatic transitions. Intra-tooth $\delta^{18}O$ profiles record seasonal conditions, summer in M2 and winter in M3, and were used to estimate past temperatures. Reconstructed mean monthly winter temperatures reached −3.1°C in layer 10, with summer temperatures rising to ~16°C in layer 9 during GI-1. These results highlight environmental continuity in red deer ecology despite climate fluctuations, suggesting that stable, open habitats supported sustained human use of the site throughout the Late Glacial.
© 2026 The Author(s). *Journal of Quaternary Science* Published by John Wiley & Sons Ltd.

KEYWORDS: carbon isotope; *Cervus elaphus*; enamel carbonate; late glacial; oxygen isotope

Introduction

The Late Glacial period (ca. 17.5–11.7 kcal a BP) was marked by abrupt climatic changes, which triggered widespread environmental transformations across Europe (Björck *et al.*, 1998; Magny et al., 2006; Ivy-Ochs et al., 2008; Lambeck et al., 2014; Monegato et al., 2015). Following the Last Glacial Maximum (LGM), the transition from cold, arid steppe landscapes to more temperate, forested environments unfolded through a series of climatic oscillations. These shifts are well documented in Greenland ice-core records and other high-resolution proxies, which capture alternating cold stadials and warmer interstadials known, respectively, as Greenland Stadial (GS) and Greenland Interstadials (GI) (Rasmussen et al., 2014). In particular, the transition from GS-2.1a to GI-1 encompasses a period of increasing climatic variability, culminating in the relatively warm Bølling–Allerød Interstadial (GI-1), followed by a return to colder conditions during the Younger Dryas (GS-1).

These climatic fluctuations shaped ecosystems across the continent, influencing the distribution of flora and fauna and the subsistence strategies of prehistoric humans. In northern and central Europe, glacial and periglacial conditions limited forest cover and reduced resource diversity, often pushing Late Palaeolithic foragers into more marginal environments (Willis et al., 2000; Magyari et al., 2014). By contrast, southern European regions, including the southern Alps, offered relatively stable and ecologically rich habitats (Monegato et al., 2015). Palynological and paleolimnological data from northeastern Italy indicate the development of boreal and open woodlands, productive wetlands, and milder microclimates, especially during the Late Glacial Interstadial (Frisia et al., 2005; Filippi et al., 2007; Heiri et al., 2007; Ravazzi et al., 2007). These favorable conditions made the southeastern Alps a key refugial zone and corridor for both fauna and human populations during a time of major climatic transition (Cusinato & Bassetti, 2007; Montoya et al., 2018).

Within this environmental setting, the Late Epigravettian culture flourished. Associated with mobile hunter-gatherer groups, the Epigravettian represents the final phase of Upper Palaeolithic in Italy, spanning from the LGM to the Pleistocene–Holocene transition. Characterized by a structured settlement system and complex subsistence strategies, Late Epigravettian groups adapted to changing ecological conditions (Bietti, 1990; Ruiz-Redondo et al., 2022). In the southern Alpine foothills, these groups exploited a diverse landscape of uplands and valley-bottoms. Faunal remains from key sites, including Riparo Tagliente, demonstrate a strong focus on red deer (*Cervus elaphus*), alongside ibex (*Capra ibex*), small mammals, and aquatic resources Fontana et al., 2009; Bertolini et al., 2016; Manzella et al., 2024). Understanding how these hunter-gatherers responded to seasonal and climatic changes requires the integration of archaeological, paleoenvironmental, and biological data.

One powerful approach to reconstructing past environmental conditions and subsistence dynamics is stable isotope

*Correspondence: D. G. Drucker, as above.
Email: dorothee.drucker@senckenberg.de

© 2026 The Author(s). *Journal of Quaternary Science* Published by John Wiley & Sons Ltd.
This is an open access article under the terms of the Creative Commons Attribution License, which permits use, distribution and reproduction in any medium, provided the original work is properly cited.

analysis of animal tooth enamel. Carbon ($\delta^{13}C$) and oxygen ($\delta^{18}O$) isotopic compositions in enamel bioapatite reflect an animal's diet and the water that it ingested during tooth formation, thus capturing signals related to vegetation type, habitat structure, and climate (Kohn et al., 1998; Koch, 2007). Under typical Late Pleistocene burial conditions, enamel carbonate is considered diagenetically robust and capable of preserving primary biogenic $\delta^{13}C$ and $\delta^{18}O$ values (e.g., Kohn and Cerling, 2002; Lee-Thorp and Sponheimer, 2003). The $\delta^{13}C$ values primarily reflect the isotopic composition of consumed plants. In C_3-dominated ecosystems such as those of Late Glacial Europe, $\delta^{13}C$ values are useful for distinguishing between open and closed environments (Tieszen, 1991; van der Merwe & Medina, 1991; Bocherens et al., 1996). Indeed, C_3 plants in dense, closed-canopy forests typically show $\delta^{13}C$ values ranging from −28‰ to −37‰, due to the higher concentration of CO_2 and low-light conditions combined with a relatively high-humidity effect (Medina et al., 1986; van der Merwe & Medina, 1989, 1991; Cerling et al., 1997). In contrast, less negative values (≥−27‰) are associated with C_3 plants from open and typically drier environments, such as grasslands or steppe areas (Bocherens, 2003). The $\delta^{18}O$ values reflect the isotopic signature of meteoric water ingested through drinking and plant moisture. Because $\delta^{18}O$ in precipitation varies seasonally and geographically, intra-tooth variation in $\delta^{18}O$ can provide insights into seasonal shifts in temperature or hydrological conditions (Kohn et al., 1998; Koch, 2007).

Among large herbivores, red deer are particularly valuable for such analyses. Ecologically adaptable and widely distributed, red deer can inhabit open steppes, forest edges, and mountainous environments. Their feeding strategy, as opportunistic mixed feeders, makes them sensitive indicators of vegetation and landscape structure (Heptner et al., 1989). Moreover, their role as a primary prey species links them directly to human foraging strategies. Interpreting $\delta^{13}C$ and $\delta^{18}O$ values in red deer enamel thus offers a dual advantage: reconstructing environmental conditions and assessing prey behavior relevant to Late Palaeolithic subsistence.

Stable isotope studies of red deer have been widely applied across Europe to explore climatic patterns, mobility, and seasonal availability of prey (e.g., Balasse et al., 2002; Stevens et al., 2011; Drucker et al., 2024). However, such applications remain limited in the eastern sector of the Italian Alps. While this biogeochemical analysis has been applied for paleodietary reconstructions from human remains (Gazzoni et al., 2013; Oxilia et al., 2021) and paleoecology studies on faunal assemblages using bulk carbon and nitrogen isotopes (Manzella et al., 2024), high-resolution enamel-based studies of red deer mobility and seasonality remain scarce. This gap is particularly striking, given the region's environmental complexity and archaeological richness during the Late Glacial.

This study addresses that gap through the analysis of $\delta^{13}C$ and $\delta^{18}O$ values in red deer molars from Riparo Tagliente, a Late Epigravettian rockshelter located in the Lessini Mountains of northeastern Italy. With a well-stratified sequence spanning the Late Glacial climatic oscillations, from the first part of the Late Glacial to the temperate Bølling–Allerød Interstadial, the site offers an ideal context for reconstructing faunal ecology and evaluating how hunter-gatherers responded to environmental change (Fontana et al., 2009, 2018; Peresani et al., 2021). The faunal assemblage is dominated by red deer, providing a solid data set for isotopic investigation. A full description of the site and stratigraphy is presented in the following section.

The objectives of this study are threefold. First, we explore dietary ecology and habitat use of red deer using $\delta^{13}C$ values, which primarily reflect vegetation structure and environmental variability during enamel formation. Second, we analyze intra-tooth $\delta^{18}O$ variability to explore seasonal signals, particularly winter–summer temperature contrasts that reflect short-term climatic conditions. Third, we interpret these isotopic signatures in the context of human subsistence strategies, considering the seasonal availability, predictability, and habitat use of red deer in shaping Late Epigravettian foraging behavior. By integrating isotopic data with archaeological and paleoecological records, this study contributes to our understanding of Late Glacial hunter-gatherer adaptations in the southern Alps. It highlights how seasonal climate patterns and landscape diversity structured the availability of key prey species and influenced human decision-making at a regional scale.

The Epigravettian sequence of Riparo Tagliente

Human presence is not documented in the Southern Alps during the LGM, with Late Gravettian and Early Epigravettian assemblages identified so far only in the eastern Berici Hills (Riparo del Broion, Trene, Paina, Stria, and Buso Doppio caves), a moderate relief located in the northern portion of the Venetian plain (Bertola et al., 2018; Peresani et al., 2021). Late Epigravettian groups reached the southern Alpine slope only after the sharp climatic and environmental changes of the LGM.

The site of Riparo Tagliente preserves the most complete Late Glacial stratigraphic sequence and provides the earliest evidence of reoccupation along the southern side of the Alps after the end of the LGM at the beginning of GS2.1a (Ravazzi et al., 2007; Fontana et al., 2009, 2018). This rockshelter is located in the village of Stallavena di Grezzana, near Verona in northeastern Italy. It lies beneath a limestone rock wall in Valpantena, a major valley in the Monti Lessini, at an altitude of 226 m above sea level (a.s.l.) (Fig. 1). Riparo Tagliente's earliest occupation predates those of the Alpine highland settlements, such as Grotta Clusantin (520 m a.s.l.), Val Lastari (1060 m a.s.l.), Riparo La Cogola (1070 m a.s.l.), Riparo Dalmeri, and Le Regole (1240 m a.s.l.), which were occupied at the onset of the temperate Bølling–Allerød Interstadial (Bertola et al., 2007). Its strategic position at the intersection of diverse topographic zones, including the plain, valley bottom, rocky slopes, and the top of the plateau, likely contributed to its repeated occupation (Bartolomei et al., 1982; Fontana et al., 2009).

The site of Riparo Tagliente was first discovered in 1958 by Mr. Francesco Tagliente (Zorzi & Mezzena, 1962), with initial excavations carried out between 1962 and 1964 by the Museo Civico di Storia Naturale di Verona. From 1967 onward, the University of Ferrara resumed and continued systematic excavations. Early research (until the mid-1970s) focused on the excavation of a long trench running transversely across the shelter to investigate the full stratigraphic sequence. This trench divides the site into two excavation sectors: southern and northern, each with an inner area sheltered by the rock wall and an exposed outer area. Excavations in the trench area reached depths of 4.6 m, revealing two major deposits separated by a river erosion. The lower deposit contains Mousterian and Aurignacian material culture (the latter only in a small internal area), whereas the upper deposit yielded abundant Late Epigravettian evidence (Fig. 1), indicating repeated occupation during the Late Glacial, and specifically during GS-2.1a and the first part of GI-1 (Bartolomei et al., 1982; Fontana et al., 2009, 2015, 2018). The Late Epigravettian sediments at Riparo Tagliente are unevenly distributed—about 100 cm thick inside the shelter and over

© 2026 The Author(s). *Journal of Quaternary Science* Published by John Wiley & Sons Ltd.

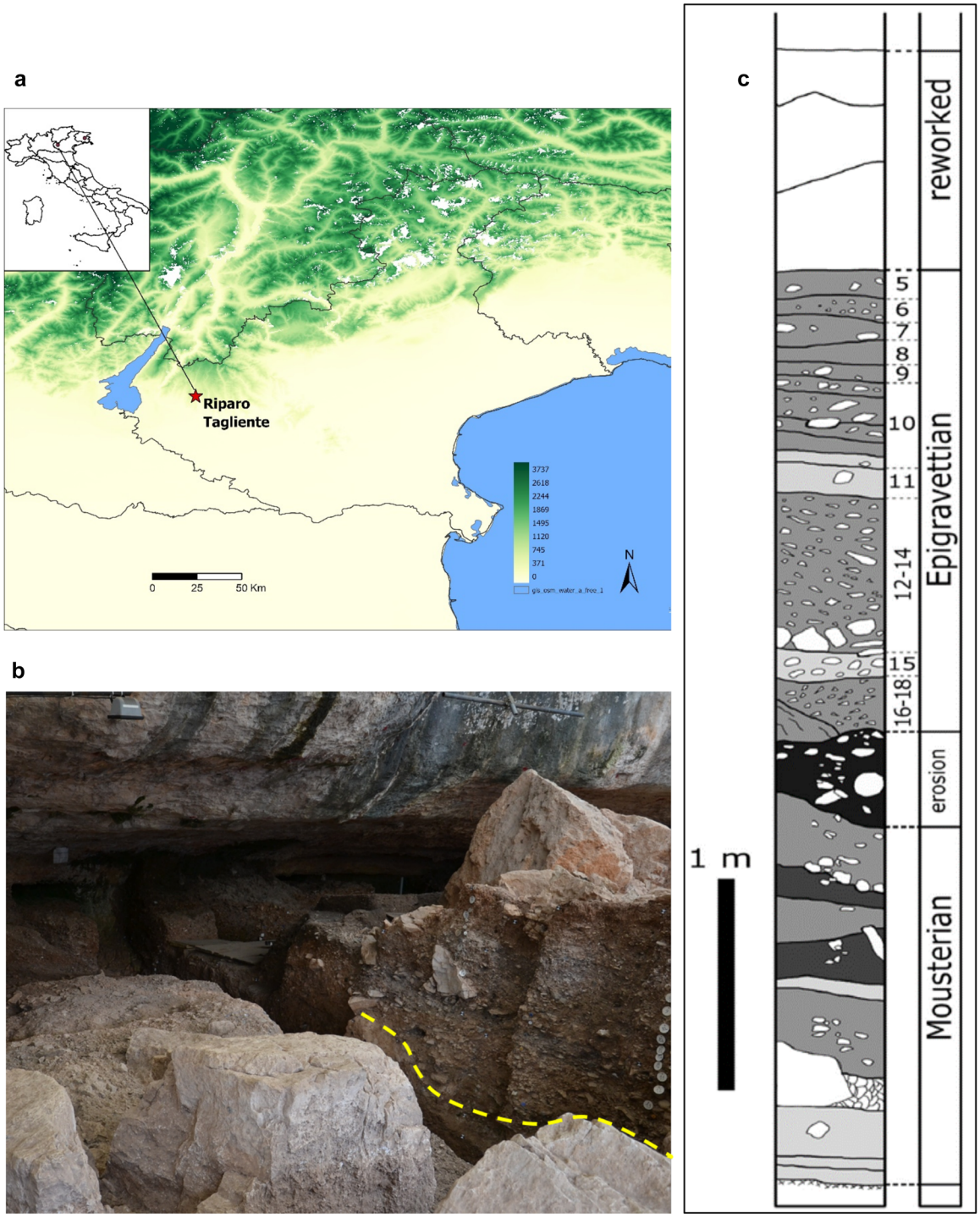

Figure 1. (a) Geographic location of Riparo Tagliente (226 m a.s.l.) in Veneto, NE Italy (ArcGIS Pro 3.2.0 elaboration by M. Amanova). (b) Stratigraphic sequence of the external trench zone. The dashed line indicates the erosion surface separating the Late Epigravettian sequence from the Mousterian and Aurignacian unit (modified from Fontana et al., 2018). (c) Stratigraphic section of the external trench. In this area, the Aurignacian levels are not detected (modified from Bartolomei et al., 1982).

2 m in the external area. This pattern is attributed to a differing site use, with inner areas kept cleaner and debris accumulating outside. Additionally, medieval excavation activities severely disturbed the inner deposits, preserving only limited portions (Bartolomei et al., 1982; Fontana et al., 2009, 2018, 2015). Overall, the Late Epigravettian sequence is characterized by an intense human activity, as reflected in the material culture, including lithic industries, dwelling structures, mobile art, ornaments (shells and animal teeth), nodules, and fragments of goethite and hematite, and an in situ burial, alongside abundant faunal remains (Bartolomei et al., 1982; Cilli et al., 2006; Fasser et al., 2022, 2024; Fontana et al., 2009; Gazzoni et al., 2013; Cavallo et al., 2017). From a sedimentological perspective, the Epigravettian deposit is divided into two subunits: a lower sequence (layers 18–15) and an upper one (layers 14–5) (Fig. 1). Both are set in a loess matrix, with the lower deposits containing denser coarse breccia than the upper ones. Multiproxy data, including sediment analysis, pollens, malacofauna, and small and large mammal remains, indicate the presence of two environmental phases. According to palynological data, the lower levels (18–15) reflect a cold, arid steppe environment, while layer 14 marks the transition to a more temperate climate with grasslands and mixed woodland (conifers and deciduous species). In layers 10d and 9,

© 2026 The Author(s). *Journal of Quaternary Science* Published by John Wiley & Sons Ltd.

broadleaves and especially *Corylus* increase (Bartolomei et al., 1982). Herbivores were a primary food resource for Late Epigravettian groups at Riparo Tagliente. Red deer is the most represented species throughout the stratigraphic sequence (number of Identified Specimens or NISP = 4522), with 52.5% of the identified specimens. First documented in layer 15, its frequency increases from levels 12 to 10, peaking in the upper layers (71.5% in layer 8). Roe deer, present from layer 14, is the second most frequent ungulate. Water-associated species such as moose (*Alces alces*) are also relatively common in layers 11–15, further indicating environmental variability during the Late Glacial period. From a stratigraphic perspective, large mammals from the lower Epigravettian layers of Riparo Tagliente (18–14) are dominated by species adapted to open and cold environments, particularly Alpine ibex (*C. ibex*) (NISP = 832), associated with *Bison* and *Bos*. In contrast, the upper levels (12–5) reflect milder conditions and an increase in temperate species such as red deer (*C. elaphus*), roe deer (*Capreolus capreolus*), and wild boar (*Sus scrofa*). Level 13 shows both faunal assemblages in roughly equal proportions (Bartolomei et al., 1982; Rocci Ris, 2006; Fontana et al., 2009). According to the latest studies of micromammal remains, the bottom layers (15–12) are dominated by *Microtus arvalis* and *Microtus* (Terricola) gr. *Multiplex-subterraneus* (over 75% of the entire assemblage). The record starts to change in Macrounit 11, where an increase in biodiversity and water component is suggested by the presence of *Arvicola amphibius,* while *M. arvalis* decreases and the attested species are more evenly distributed in the assemblage without a dominating one, probably reflecting an increase in woodland and water components. Nevertheless, the two uppermost Macrounits (layers 8–9 and 5–7) have a low MNI with an assemblage dominated by *M. arvalis*, and, thus, characterized by a low biodiversity. Overall, the climate reconstruction based on small mammals from Riparo Tagliente indicates an increase in temperatures (especially MAT and MTW) starting from layer 11. However, throughout this warming-up phase, the assemblage continues to record relative stability of the open environments in Valpantena, along the southern Alpine fringe (Berto et al., 2018).

Radiocarbon dating performed on human remains, charcoals, and animal bones from the Epigravettian layers indicates that the sequence spans from approximately 17.2 k cal a BP (layer 13a alpha) to 13.4 k cal a BP (layers 8–10), placing the Late Epigravettian unit of Riparo Tagliente among the most complete in northern Italy (Fig. 2) (Fontana et al., 2018). For the oldest layers, radiocarbon dating performed on charcoal remains from the trench area (layers 15–16) in the 1980s indicates a time span between 16.8 and 15.5 k cal a BP. This age is superseded by more recent dating of animal bones from the bottom layers of the inner area (Northern sector, layers 13a alpha and 300), which span 17.2–16.6 k cal a BP. Meanwhile, a date from layer 13a (16 438–15 941 cal a BP) is in close agreement with those from the trench. All these dates clearly locate the bottom layers of Riparo Tagliente in early Oldest Dryas (GS-2.1a) (Fontana et al., 2018). The dates from the burial and a human mandible associated with the same individual refer to the same time range: rib and femur of Tagliente 1 yielded an age of 16 130–15 570 cal a BP and 16 460–16 130 cal a BP, respectively; molar of Tagliente 2 has been radiocarbon dated to 16 980–16 500 cal a BP (Gazzoni et al., 2013; Bortolini et al. 2021; Yavuz et al., 2024). Pending the new radiometric datings currently in progress and relying, for the moment, on the old dates obtained from charcoals found in the trench, the transition between the Oldest Dryas and the Late Glacial Temperate Interstadial (GI-1c1) would occur in correspondence to layers 10-8 (14 535–13 472 cal a BP). Moreover, the dates obtained from animal bones in levels 10e and 10c in the 1990s seem to place these levels in the final phase of the Oldest Dryas (16.5–15.2 k cal a BP), with the date from 10a marking the transition (15 537–14 243 cal a BP). One dating is considered unreliable for its wide standard deviation

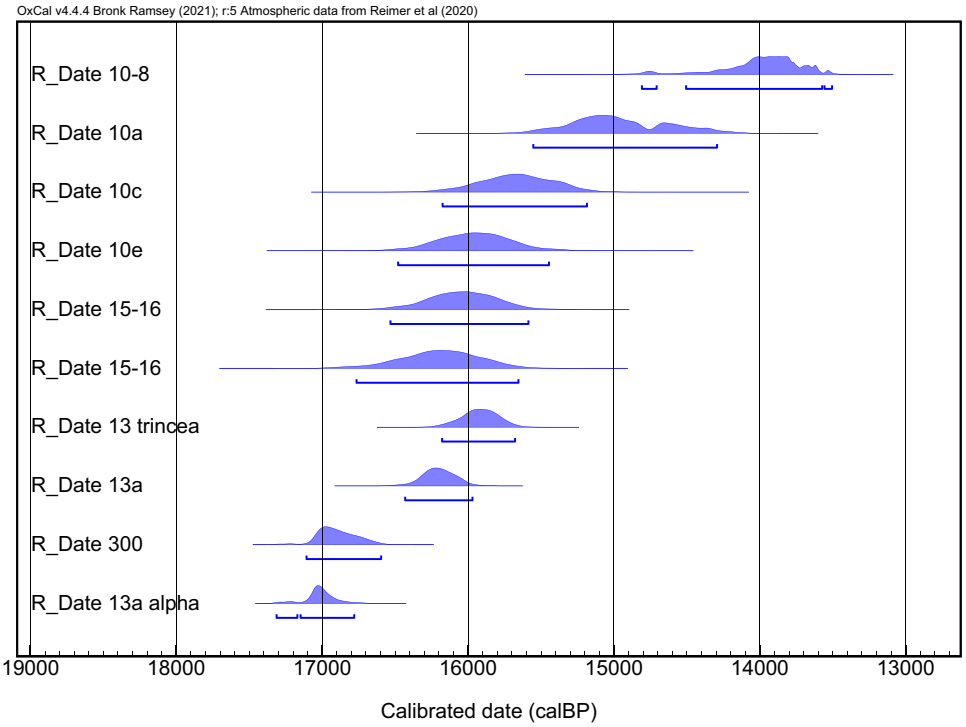

Figure 2. Plot of the radiocarbon dates for the stratigraphically coherent units of Riparo Tagliente. Layers 10–8 to 15–16 (upper part) correspond to samples from the trench area and were dated before the 2000s; layers 13 (trincea), 13a, 300, and 13aα were dated after the 2000s and derive from samples recovered during extensive excavations in the northern sector. Ages are calibrated with OxCal 4.4 software (Bronk Ramsey, 2021) using the IntCal20 curve (Reimer *et al.*, 2020).

© 2026 The Author(s). *Journal of Quaternary Science* Published by John Wiley & Sons Ltd.

(layer 14: 15 271–13 095 cal a BP), while those from layers 352 (16 638–16 179 cal a BP) and 419 (14 966–14 175 cal a BP) do not correspond to their stratigraphic position, making them either older or younger than expected (Fontana et al., 2018). For clarity, the plot shown in Fig. 2 includes only the dates considered reliable from both the trench area and the Northern sector.

Materials and methods

Material selection

Dental material can serve as a chronological record of an individual's diet over a specific period of life as well as of the associated climatic conditions. To reconstruct the seasonal change in the diet and habitat of the red deer from Riparo Tagliente, sample selection focused on the latest-forming permanent third molar (M3) and, whenever possible, the second permanent molar (M2). The seasonal changes recorded in the enamel correspond to the duration of the crown formation (mineralization) of the teeth (e.g., Balasse et al., 2003). The mineralization period of teeth in herbivores begins prior to tooth eruption and is fully completed before the eruption process concludes (Kohn et al., 1998; Kohn & Cerling, 2002). Red deer's second molars erupt between 12 and 16 months, and third molars erupt between 21 and 32 months after birth (Godawa, 1989; Brown & Chapman, 1991a; Azorit et al., 2002). Based on the radiographic observations of modern red deer jawbone by Brown & Chapman (1991b), the mineralization of the second molar in red deer takes place between 3 and 9 months, and the third molar between 9 and 26 months. Therefore, the second molars should provide a record of one summer and/or winter of the first year and the third molars should provide a record of the whole one-year season of the second year of life. It should be noted that mineralization of the second molar theoretically overlaps with the pre-weaning period (6–8 months; Clutton-Brock et al., 1982), during which the consumption of maternal milk can result in an ^{18}O-enriched body-water signal (Stevens et al., 2011).

The collected teeth come from the upper stratigraphic units of Riparo Tagliente, dated to the Late Epigravettian (Bartolomei et al., 1982; Fontana et al., 2009). Namely, they belong to the following layers (or *tagli* as they were originally named): 5, 6, 7, 7b, 8, 9, 10a, 10b, 10c, 10d, and 13. We excluded the specimens from uppermost layers (1, 4, 4a, and 4b), which were reworked in ancient times and could not be attributed to a specific phase of occupation. We did not have any adequate samples from layers 11, 12, and 14. Depending on the archaeological layer, either the right or left M3 was systematically selected to ensure that different individuals were represented and to avoid analyzing the same individual more than once. Since only the third molar can be safely identified for isolated teeth, some associated M2 could be sampled only when they were still enclosed in the jawbone. We aimed at selecting and sampling only intact teeth, avoiding breaks and large fractures, since they might contain potential diagenetic carbonates that can contaminate our samples for isotope analysis. In total, 42 red deer teeth, i.e., 33 lower third molars and 9 lower second molars, were selected for carbonate (CO_3) isotopic analysis (see Table 1 for details). The dental enamel of these lower molars was analyzed for stable oxygen ($^{18}O/^{16}O$) and carbon ($^{13}C/^{12}C$) isotope ratios.

Sampling of materials

Enamel sampling was performed on the buccal (labial) side of the teeth, which provides a smooth and accessible area where the enamel is relatively thick, as it is standard practice in high-resolution isotopic studies (e.g., Price et al., 2017; Stevens et al., 2011). One tooth (RPT-36) was sampled differently because the buccal surface was affected by a wide crack. The M3 was sampled on the mesial (anterior) or middle loph (e.g., Fig. 3). Whenever possible, sampling was performed on the distal (posterior) loph of the M2 that is adjacent to the mesial loph of M3, which might help record a more extended seasonal sequence.

Teeth enamel surfaces were mechanically cleaned using a diamond-coated drill bit to remove adhering sediments and surface contaminants. The drill bit was periodically rinsed with Milli-Q water to prevent cross-contamination, and no chemical cleaning agents were used. A series of horizontal bands of enamel were then collected along the crown using the diamond-coated drill bit. These successive bands were sampled from the top to the bottom of the crown, that is, from the occlusal surface to the enamel–root junction (ERJ) (e.g., Fig. 3). The ERJ point was used as a reference point for measurement of the band distances (reported in the plotted graphs). In the case of an isolated tooth without a preserved root or a tooth still embedded in the jawbone, the reference point 0 corresponds to the visible bottom part of the crown. Between 11 and 5 bands per tooth were obtained from molars M3 and M2, whose crowns' heights range from 27.6 to 12.7 mm. For each sampled band, about 10–15 mg of enamel powder was cautiously collected, avoiding the underlying dentine, which could induce isotopic alteration in the enamel bioapatite. In addition, 18–20 mg of dentine powder was also collected only from third molars to control the quality of the isotope analysis of the samples. A total of 303 sample tubes of enamel and 31 of root dentine were prepared for the pre-treatment phase (Table 1).

Carbonate pre-treatment

The pre-treatment procedure of the samples was carried out following the protocol used at the laboratory of the working group Biogeology from the Department of Geosciences of the University of Tübingen. The pre-treatment phase involved adding 1.35 mL of sodium hypochlorite (NaOCl) at a concentration of 2.5% to enamel powder samples to remove the organic composition. Then, samples were placed on a shaking plate (Heidolph Vibramax 100) for 24 h. The next day, vials were centrifuged for 5 min at 5000 rpm (ca. 2430 x g) to separate liquids from solids, after which the NaOCl (2.5% Cl) solution was removed, and samples were rinsed three times with Millipore water (Milli-Q H2O) to wash NaOCl off. This step was repeated twice for the dentine samples. Afterward, to remove all the diagenetic carbonates, the samples were reacted with 1M acetic acid-buffered solution (CH_3COOH) for 24 h (e.g., Koch et al., 1997; Wright & Schwarcz, 1998; 1999). As on day one, the samples were again placed on the shaking plate at 450 rpm for 24 h. The process on the last day consisted of centrifugation, removing the buffered solution, which was also accompanied by rinsing three times with Milli-Q water. In the end, the samples were allowed to dry in an oven set at 35°C for 72 h.

IRMS measurement

The isotope compositions of pretreated enamel (carbonates) were measured using the isotope ratio mass spectrometry (IRMS) in the Senckenberg Centre for Human Evolution and Palaeoenvironment at the University of Tübingen. For IRMS, we took 2.5–3.0 mg of carbonates, dentine samples, and in-lab standards (enamel of elephant and hippo fossils from Chad),

© 2026 The Author(s). *Journal of Quaternary Science* Published by John Wiley & Sons Ltd.

Table 1. Final list of the selected teeth of red deer (*Cervus elaphus*).

Lab ID	Excavation ID	SU	Tooth		Bands N	ERJ point	Crown height (mm)
RPT-R6	RT81 Q35/9 #9138	5	Lower M3	Left	7	Yes	23.5
RPT-R7	RT q20/4 #6574	5	Lower M3	Left	5	No	17.6
RPT-R8	RT q631 #6757	6	Lower M3	Right	8	Yes	21.1
RPT-R9	RT81 q50/5 #9488	6	Lower M3	Left	7	No	18.0
RPT-R10	RT81 q50/6 #9475	6	Lower M3	Left	6	Yes	16.6
RPT-R11	RT q23 #7001	7b	Lower M3	Right	9	Yes	23.2
RPT-R12	RT q9 #6920	7	Lower M3	Right	10	Yes	24.0
RPT-R13	RT81 q21/8	7	**Lower M2**	Right	8	Yes	15.5
RPT-R13	RT81 q21/8	7	Lower M3	Right	8	Yes	19.1
RPT-R14	RT q6 #6839	7	Lower M3	Right	7	Yes	18.6
RPT-R15	RT81 q35/7 #7002	7	Lower M3	Right	8	Yes	19.3
RPT-R16	RT q6 #6850	7	**Lower M2**	Right	5	No	12.7
RPT-R16	RT q6 #6850	7	Lower M3	Right	6	No	13.0
RPT-17	RT62 Q20/7 #7636	8	Lower M3	Right	8	Yes	20.7
RPT-18	RT8 q6 #7628	8	**Lower M2**	Right	9	No	17.3
RPT-18	RT8 q6 #7628	8	Lower M3	Right	8	Yes	21.1
RPT-19	RT Q36/3 #7643	8	**Lower M2**	Right	6	Yes	16.6
RPT-19	RT Q36/3 #7643	8	Lower M3	Right	6	Yes	18.6
RPT-20	RT Q6 #7556	8	**Lower M2**	Right	5	Yes	14.0
RPT-20	RT Q6 #7556	8	Lower M3	Right	7	Yes	15.8
RPT-21	RT Q80/9 #9727	9	**Lower M2**	Right	5	Yes	14.1
RPT-21	RT Q80/9 #9727	9	Lower M3	Right	6	Yes	13.0
RPT-22	RT Q23 #8512	9	**Lower M2**	Right	5	Yes	13.7
RPT-22	RT Q23 #8512	9	Lower M3	Right	6	Yes	14.7
RPT-23	RT Q64/5-8 #8536	9	Lower M3	Right	9	Yes	21.5
RPT-24	RT Q6 #9526	9	**Lower M2**	Right	9	Yes	19.0
RPT-24	RT Q6 #9526	9	Lower M3	Right	8	Yes	18.9
RPT-25	RT Q19/4 #1181	10a	Lower M3	Left	7	Yes	16.7
RPT-26	RT Q35/6 #1176	10a	Lower M3	Right	6	Yes	17.5
RPT-27	RT Q22	10a	**Lower M2**	Right	6	Yes	15.5
RPT-27	RT Q22	10a	Lower M3	Right	7	Yes	17.9
RPT-36	RT Q22 #3055	10a	Lower M3	Right	6	Yes	21.2
RPT-37	RT Q54 #1302	10a	Lower M3	Right	9	Yes	27.6
RPT-38	RT Q35/9 #1191	10a	Lower M3	Right	6	Yes	18.9
RPT-28	RT Q38/6 #1198	10b	Lower M3	Right	7	Yes	17.5
RPT-29	RT Q80/7 #1237	10b	Lower M3	Right	11	Yes	22.3
RPT-30	RT Q37/6 #1166bis	10c	Lower M3	Right	8	Yes	23.2
RPT-31	RT Q50 #1229	10d	Lower M3	Right	8	Yes	22.8
RPT-32	RT Q79/9 #1239	10d	Lower M3	Right	8	Yes	19.1
RPT-33	RT Q15 #4727	13	Lower M3	Left	8	Yes	23.7
RPT-34	RT Q511-7 #4118	13	Lower M3	Left	7	Yes	21.1
RPT-35	RT Q15 #4695	13	Lower M3	Left	8	Yes	18.2
Total					**303**		

Note: The ***total -303*** is the number of enamel samples prepared for isotope analysis.
Abbreviations: ERJ, Enamel–Root Junction; M2, second molar; M3, third molar; SU, Stratigraphic Unit.

which were subjected to the same pretreatment as the other enamel samples. Vials with carbonates were then placed in the heated sample tray in the MultiFlow-Geo preparation system, where they were reacted with highly concentrated (~99%) phosphoric acid (H_3PO_4) at 70°C for 4 h. From this equilibration, the carbonate was obtained as CO_2 gas and sent through the MultiFlow-Geo system to the Elementar IsoPrime100 IRMS, where CO_2 was measured four times within 15 min to obtain the isotopic values.

Measured isotopic ratios are reported as mean values that were calibrated with two international standards (IAEA-603 with $\delta^{13}C = +2.46‰$ and $\delta^{18}O = -2.37‰$ and NBS-18 with $\delta^{13}C = -5.01‰$ and $\delta^{18}O = -23.20‰$) using "LyticOS" software. Additionally, three in-house standards (pure carbonate Laaser Marmor with $\delta^{13}C = +1.50‰$ and $\delta^{18}O = -5.20‰$, elephant with $\delta^{13}C = -10.55‰$ and $\delta^{18}O = +1.80‰$, and hippo with $\delta^{13}C = -3.80‰$ and $\delta^{18}O = -2.10‰$) were analyzed alongside to monitor accuracy and precision. The final carbonate $\delta^{13}C_{carb}$ and $\delta^{18}O_{carb}$ mean values obtained from the IRMS measurements are presented versus the VPDB standard (in ‰). In addition, $\delta^{18}O_{carb}$ values in VPDB were also converted into the VSMOW scale (in ‰) using the following equation of Coplen (1988):

$$\delta^{18}O_{VSMOW} = (1.03091 \times \delta^{18}O_{VPDB}) + 30.91 \quad (3.1)$$

The measurement uncertainty was monitored using three in-house standards. The overall analytical precision is better than 0.1‰ for carbon ($\delta^{13}C$) and better than 0.2‰ for oxygen ($\delta^{18}O$) isotopic values.

The carbonate (CO3) content is calculated based on peak area versus weight of carbonate sample scaled up to 100% CO3 for IAEA and NBS standards, and 5.1% CO3 for the hippo enamel.

Calculation methods for air temperature (T_{air})

To calculate temperatures recorded by the red deer teeth during summer and winter, we converted the measured minimum and maximum $\delta^{18}O_{carb}$ values along sinusoidal curves into $\delta^{18}O$ values of drinking water consumed by the red

© 2026 The Author(s). *Journal of Quaternary Science* Published by John Wiley & Sons Ltd.



Figure 3. Lower M3R—after sampling (sampled buccal side).

deer to compare the tooth $\delta^{18}O_{carb}$ isotope signatures to modeled precipitation $\delta^{18}O$. Following the equation of Iacumin et al. (1996), the drinking water $\delta^{18}O_W$ of the Riparo Tagliente red deer was calculated as follows:

$$\delta^{18}O_{carb} = (0.998 \times \delta^{18}O_W) + 33.63 \quad (3.2)$$

Since the main source of drinking water consumed by ungulates is supplied by precipitation, we converted the $\delta^{18}O_W$ values into air temperature (T_{air}). Seasonal variations in red deer intra-tooth $\delta^{18}O_{carb}$ isotope values reflect seasonal climatic variability; therefore, temperature reconstruction requires equations that relate $\delta^{18}O_W$ values to the mean monthly temperature (MMT).

For regional-scale paleotemperature reconstruction, we applied a European-scale transfer model following Reiss et al. (2024). This model is based on long-term GNIP records from 84 meteorological stations distributed across Europe and uses the mean monthly temperatures of the warmest months (July–August) and coldest months (December–January) to represent summer and winter conditions, respectively. Summer and winter air temperatures were calculated using the following equations:

$$T_{summer} = (\delta^{18}O_{precipitation} + 15.66)/0.50 \quad (3.3)$$

$$T_{winter} = (\delta^{18}O_{precipitation} + 11.74)/0.53 \quad (3.4)$$

It should be noted that temperature reconstructions based on $\delta^{18}O$ values, while derived from established empirical relationships, rely on several simplifying assumptions. Moreover, enamel growth patterns lead to a dampening of seasonal extremes in the isotopic signal (e.g., Passey and Cerling, 2002). Consequently, the resulting temperature estimates should be regarded as approximate and indicative rather than absolute values.

Results

Enamel carbonate quality control

In this study, the overall carbonate content in enamel samples ranges from 2.5% to 4.9%, while dentine samples show a broader range from 1.5% to 6.4% (Table A1). Intra-tooth variation in CO_3 weight percent ranges between 0.1% and 1.8% for enamel samples (Fig. A1).

Prior to compiling a reliable isotopic data set, all enamel samples were assessed for carbonate content quality control (QC). QC was applied only to teeth showing intra-tooth CO_3 variability greater than analytical precision, defined here as a standard deviation (SD) equal to or greater than 0.4%. For these teeth, individual carbonate bands were evaluated against an acceptable range defined as mean $(CO_3) \pm$ SD, and bands falling outside this range were excluded. Teeth with CO_3 standard deviations below 0.4% were considered internally consistent and were not subjected to band-level exclusion. Exclusion of carbonate bands resulted in the removal of the corresponding $\delta^{13}C$ and $\delta^{18}O$ values prior to further isotopic interpretation. Fig. A2 illustrates isotopic profiles before and after carbonate (CO_3) quality control.

Following application of the QC criteria, only 10 teeth showed CO_3 standard deviations ≥0.4%. From these samples, a total of 15 carbonate bands falling outside the accepted range were removed. One exception concerns the third molar of specimen RPT-R11 (layer 7), in which a single band displaying an anomalously low isotopic $\delta^{18}O$ value was excluded despite not meeting the formal carbonate QC threshold (Fig. A2). It should be noted that dentine can induce isotopic alteration in enamel bioapatite, typically increasing carbonate content and $\delta^{18}O$ values; however, such an effect is not observed in this sample.

Carbonate $\delta^{13}C$ isotopic results

The $\delta^{13}C_{carb}$ values for all analyzed teeth were similar and ranged from –13.3‰ to –10.7‰ in the entire stratigraphic sequence of the Late Epigravettian at Riparo Tagliente (Table 2). The mean $\delta^{13}C_{carb}$ values per tooth varied from –12.8‰ to –11.2‰, with a standard deviation between 0.1‰ and 0.5‰, reflecting intra-tooth variability among sequential enamel bands. Only one red deer tooth, RPT-29 from level 10b, had a lower mean $\delta^{13}C_{carb}$ value (also in $\delta^{18}O_{carb}$), whereas the values of the rest of the specimens ranged between –12.5‰ and –11.2‰ on average (Fig. A4).

The intra-tooth $\Delta\delta^{13}C_{carb}$ variability in teeth (that is, a difference between the highest and lowest values per tooth)

© 2026 The Author(s). *Journal of Quaternary Science* Published by John Wiley & Sons Ltd.

Table 2. Summary statistics results of carbonate $\delta^{13}C$ and $\delta^{18}O$ isotope values for each red deer tooth.

					(‰ VPDB)					(‰ VSMOW)				
Lab ID	Excavation ID	SU	Tooth	N	$\delta^{13}C_{carb}$ Min	Max	Range	Mean	SD	$\delta^{18}O_{carb}$ Min	Max	Range	Mean	SD
RPT-R6	RT81 Q35/9 #9138	5	M3 L	7	−12.1	−11.8	0.3	−11.9	0.1	**22.6**	25.2	2.6	23.8	1.0
RPT-R7	RT q20/4 #6574	5	M3 L	5	−12.5	−11.6	0.9	−12.0	0.4	25.3	26.6	1.3	25.7	0.6
RPT-R8	RT q631 #6757	6	M3 R	8	−11.6	−10.7	0.8	−11.3	0.3	**21.8**	24.5	2.7	22.9	1.0
RPT-R9	RT81 q5015 #9488	6	M3 L	7	−12.4	−12.1	0.4	−12.3	0.2	23.3	24.5	1.2	23.8	0.5
RPT-R10	RT81 q50/6 #9475	6	M3 L	5	−11.2	−11.1	0.2	−11.2	0.1	**23.4**	25.3	1.8	24.5	0.7
RPT-R11	RT q23 #7001	7b	M3 R	8	−11.8	−11.3	0.6	−11.6	0.2	**23.1**	26.1	3.0	24.4	1.2
RPT-R12	RT q9 #6920	7	M3 R	10	−12.4	−10.8	1.5	−11.6	0.5	23.0	24.1	1.1	23.4	0.4
RPT-R13	RT81 q21/8	7	**M2 R**	8	−11.6	−10.9	0.7	−11.2	0.2	23.5	26.4	2.9	25.6	1.0
RPT-R13	RT81 q21/8	7	M3 R	8	−12.0	−11.3	0.8	−11.7	0.2	**23.2**	25.3	2.1	24.0	0.7
RPT-R14	RT q6 #6839	7	M3 R	7	−12.7	−12.2	0.5	−12.5	0.2	23.6	25.0	1.3	24.4	0.7
RPT-R15	RT81 q35/7 #7002	7	M3 R	5	−11.8	−11.6	0.3	−11.7	0.1	**22.6**	24.7	2.1	23.6	0.8
RPT-R16	RT q6 #6850	7	**M2 R**	5	−12.7	−12.1	0.6	−12.4	0.2	22.8	25.3	2.5	24.0	1.1
RPT-R16	RT q6 #6850	7	M3 R	6	−12.3	−11.9	0.4	−12.1	0.2	23.4	24.0	0.6	23.7	0.3
RPT-17	RT62 Q20/7 #7636	8	M3 R	8	−11.6	−10.9	0.8	−11.2	0.2	**22.2**	25.2	3.0	23.6	1.1
RPT-18	RT8 q6 #7628	8	**M2 R**	6	−11.6	−11.0	0.6	−11.5	0.2	21.1	24.6	3.5	22.2	1.2
RPT-18	RT8 q6 #7628	8	M3 R	7	−12.6	−11.5	1.1	−12.0	0.4	23.1	24.7	1.7	24.0	0.6
RPT-19	RT Q3613 #7643	8	**M2 R**	6	−12.6	−12.1	0.5	−12.4	0.2	22.8	24.9	2.1	23.7	0.9
RPT-19	RT Q36/3 #7643	8	M3 R	6	−12.4	−11.5	1.0	−11.9	0.3	24.0	24.8	0.8	24.3	0.3
RPT-20	RT Q6 #7556	8	**M2 R**	5	−12.3	−11.7	0.6	−12.0	0.2	23.5	24.9	1.4	24.3	0.6
RPT-20	RT Q6 #7556	8	M3 R	6	−12.3	−11.8	0.4	−12.1	0.2	23.3	24.6	1.3	24.0	0.4
RPT-21	RT Q80/9 #9727	9	**M2 R**	5	−12.1	−11.8	0.3	−12.0	0.1	24.4	26.6	2.3	25.3	1.0
RPT-21	RT Q80/9 #9727	9	M3 R	6	−12.0	−11.4	0.6	−11.8	0.2	22.2	24.9	2.7	23.6	0.9
RPT-22	RT Q23 #8512	9	**M2 R**	5	−12.5	−11.5	1.0	−12.0	0.4	22.3	25.7	3.4	24.1	1.4
RPT-22	RT Q23 #8512	9	M3 R	6	−11.9	−11.1	0.8	−11.4	0.3	23.2	25.7	2.4	24.5	0.9
RPT-23	RT Q64/5-8 #8536	9	M3 R	9	−12.2	−11.1	1.1	−11.7	0.4	23.0	**26.1**	3.2	24.9	1.1
RPT-24	RT Q6 #9526	9	**M2 R**	6	−12.2	−11.8	0.4	−12.0	0.1	24.1	26.6	2.5	25.2	0.7
RPT-24	RT Q6 #9526	9	M3 R	8	−12.4	−12.1	0.3	−12.2	0.1	23.2	**26.2**	2.9	24.8	1.0
RPT-25	RT Q19/4 #1181	10a	M3 L	5	−12.1	−11.7	0.4	−11.9	0.1	21.2	24.4	3.2	23.3	1.1
RPT-26	RT Q35/6 #1176	10a	M3 R	6	−12.4	−11.9	0.5	−12.1	0.2	22.0	**25.2**	3.2	23.9	1.3
RPT-27	RT Q22	10a	**M2 R**	6	−12.6	−12.0	0.6	−12.3	0.3	22.6	24.8	2.2	23.9	0.9
RPT-27	RT Q22	10a	M3 R	7	−11.6	−11.0	0.6	−11.4	0.2	23.7	24.4	0.7	23.9	0.2
RPT-28	RT Q38/6 #1198	10b	M3 R	7	−11.3	−11.0	0.3	−11.2	0.1	23.7	25.5	1.8	24.4	0.6
RPT-29	RT Q80/7 #1237	10b	M3 R	11	−13.3	−12.3	1.1	−12.8	0.4	**20.3**	22.6	2.3	21.2	0.7
RPT-30	RT Q37/6 #1166bis	10c	M3 R	8	−11.9	−11.1	0.7	−11.5	0.2	**21.8**	**24.4**	**2.6**	23.1	1.0
RPT-31	RT Q50 #1229	10d	M3 R	8	−11.7	−10.8	0.9	−11.3	0.3	22.2	23.9	1.7	23.0	0.6
RPT-32	RT Q79/9 #1239	10d	M3 R	8	−12.2	−11.8	0.4	−12.0	0.1	**21.0**	23.1	2.1	21.8	0.8
RPT-36	RT Q22 #3055	10a	M3 R	6	−11.7	−11.5	0.3	−11.6	0.1	**21.1**	23.6	2.4	21.8	0.9
RPT-37	RT Q54 #1302	10a	M3 R	9	−12.0	−11.3	0.6	−11.6	0.2	**20.4**	23.8	3.4	21.9	1.1
RPT-38	RT Q35/9 #1191	10a	M3 R	6	−12.6	−11.6	1.0	−12.1	0.3	20.5	23.8	3.4	22.0	1.2
RPT-33	RT Q15 #4727	13	M3 L	8	−11.8	−11.0	0.7	−11.4	0.2	21.5	24.1	2.6	22.6	0.9
RPT-34	RT Q511-7 #4118	13	M3 L	7	−11.6	−10.9	0.7	−11.2	0.3	20.9	22.8	1.9	22.0	0.7
RPT-35	RT Q15 #4695	13	M3 L	8	−12.2	−11.1	1.1	−11.8	0.3	22.9	23.5	0.5	23.2	0.2

Note: Minimum (Min), maximum (Max), mean and standard deviation (SD) of $\delta^{13}C_{carb}$ and $\delta^{18}O_{carb}$ values per tooth. Numbers in bold indicate the seasonal contrast, winter (Min) and summer (Max), detected in the profiles of the $\delta^{18}O_{carb}$ values. All teeth are lower permanent second molars (M2) and third molars (M3).
Abbreviations: L, left side; N, number of analyzed samples (bands) per tooth; R, right side; SU, stratigraphic unit.

ranged from 0.1‰ to 1.5‰ (Table 2). Out of 33 third molars, only one specimen RPT-R12 showed an inverted *U*-shaped pattern (layer 7) and four specimens RPT-R7, RPT-R16, RPT-30, and RPT-35 generated a sinusoidal pattern in $\delta^{13}C_{carb}$ values (Fig. A2). Twenty specimens displayed quite flat profiles or unclear tendency, with a range of values of less than 1‰ (0.3‰ to 0.9‰), with the rest have slightly sloping profiles that tended toward either winter (RPT-R8, RPT-29, RPT-34, and RPT-38) or summer (RPT-18, RPT-19, RPT-22, and RPT-23) seasons. From the set of second molars, three (RPT-19, RPT-20, and RPT-27) showed a slight reflection of the summer season effect, although they have not completed the incremental curves (Fig. A2). One specimen (RPT-22) produced an unclear profile in $\delta^{13}C_{carb}$ values, with a range value of 1.0‰. Finally, the rest of the second molars generated more flat models than seasonal fluctuations, with intra-tooth variability ranging from 0.1‰ to 0.7‰ (Fig. A2).

The $\delta^{13}C_{carb}$ values varied from –13.3‰ to –10.7‰ in all third molars and ranged between –12.7‰ and –10.9‰ in all second molars. The $\delta^{13}C_{carb}$ values of these second molars are slightly higher than the corresponding third molars, which showed $\delta^{13}C_{carb}$ values between –12.9‰ and –11.0‰ (Table 2). This supports a slight change in the summer–winter diet and/or environment within the specimen. Red deer (RPT-27) from level 10a had $\delta^{13}C_{carb}$ values ranging from –11.6‰ to –11.0‰ in the third molar, which were higher than –12.6‰ and –12.0‰ in the second molar. This should confirm a significant difference between summer (second molar) and winter (third molar), although the $\delta^{18}O_{carb}$ values provided a flat profile where no seasonal tendency could be seen. Red deer from other stratigraphic layers, for which both second and third molars were sampled, did not provide as high an inter-tooth (M3 and M2) variation in $\delta^{13}C_{carb}$ values as in level 10a (Table 2).

© 2026 The Author(s). *Journal of Quaternary Science* Published by John Wiley & Sons Ltd.

Considering all samples (42 teeth), red deer did not show a significant difference in $\delta^{13}C_{carb}$ values when grouped according to the stratigraphic units. However, the graph plotted based on the mean values of $\delta^{13}C_{carb}$ and $\delta^{18}O_{carb}$ still showed that there are some red deer teeth with relatively high $\delta^{13}C_{carb}$ values in layers 13 and 10b, as well as in the upper layers 8, 7, and 6. Moreover, the lowest mean $\delta^{13}C_{carb}$ values were observed in the specimens from layer 10b together with layers 7 and 8 (Fig. A4).

Carbonate $\delta^{18}O$ isotopic results

The $\delta^{18}O_{carb}$ isotopic values ranged from +20.3‰ to +26.6‰ when considering all red deer teeth (Table 2). The intra-tooth range of $\delta^{18}O_{carb}$ values spanned from 0.5‰ to 3.5‰, which is much higher than those in $\delta^{13}C_{carb}$, as expected with seasonal fluctuations of temperature. The observed seasonal patterns in $\delta^{18}O_{carb}$ values were mainly isolated winter or summer signals, and some complete seasonal cycles (winter and summer) (Fig. 4). Incremental $\delta^{18}O_{carb}$ profiles were grouped into a limited number of curve types reflecting different degrees of seasonal completeness (Table A2; Figs. A2 and A3). Thirteen teeth displayed unclear or incomplete trends, likely reflecting partial crown preservation or reduced crown height (e.g., 12.7 mm in RPT-R16-M2) or limited sampling resolution. Flat profiles ($n = 4$) showed no detectable seasonal variation. Only three specimens recorded a complete sinusoidal pattern, capturing both summer and winter signals. *U*-shaped profiles ($n = 9$) and reversed *J*-shaped profiles ($n = 4$) primarily reflect winter-dominated signals, whereas nine specimens showed summer-dominated profiles characterized by inverted *U*-shaped or partially developed curves. As a result, only the maximum and minimum $\delta^{18}O_{carb}$ values corresponding to summer and winter phases in third molars are shown in the plotted graph (Fig. 5a), which are subsequently used to calculate the mean monthly temperature (MMT). To evaluate whether the $\delta^{13}C_{carb}$ data support these seasonal signals, the corresponding $\delta^{13}C_{carb}$ values were grouped and analyzed. Slightly elevated $\delta^{13}C_{carb}$ values were observed in layers 8 and 6, while layers 10 and 9 also showed slightly higher values in summer phases (Fig. 5b).

Overall, twelve third molars clearly reflected a winter seasonal signal, while only four specimens showed a summer season. Among the second molars, four effectively recorded the sole summer period and two showed a winter signal (Fig. A2). A couple of third molars (RPT-R12 and RPT-35) provided an unclear trend in $\delta^{18}O_{carb}$ values, while they recorded a seasonal signal in $\delta^{13}C_{carb}$ values (–12.4‰ to –10.8‰ and –12.2‰ to –11.1‰, respectively), reflecting the winter season. In five specimens, the summer season in $\delta^{18}O_{carb}$ pattern was coeval to lower $\delta^{13}C_{carb}$ values (M3 = RPT-18, RPT-23, RPT-26; M2 = RPT-20, RPT-27). In most teeth (M3 and M2) that reflected only winter in the $\delta^{18}O_{carb}$, the range in $\delta^{13}C_{carb}$ values was less than 1.0‰, with a slight increase in $\delta^{13}C_{carb}$ values in five teeth (RPT-17, RPT-19-M2, RPT-34, RPT-36, and RPT-37).

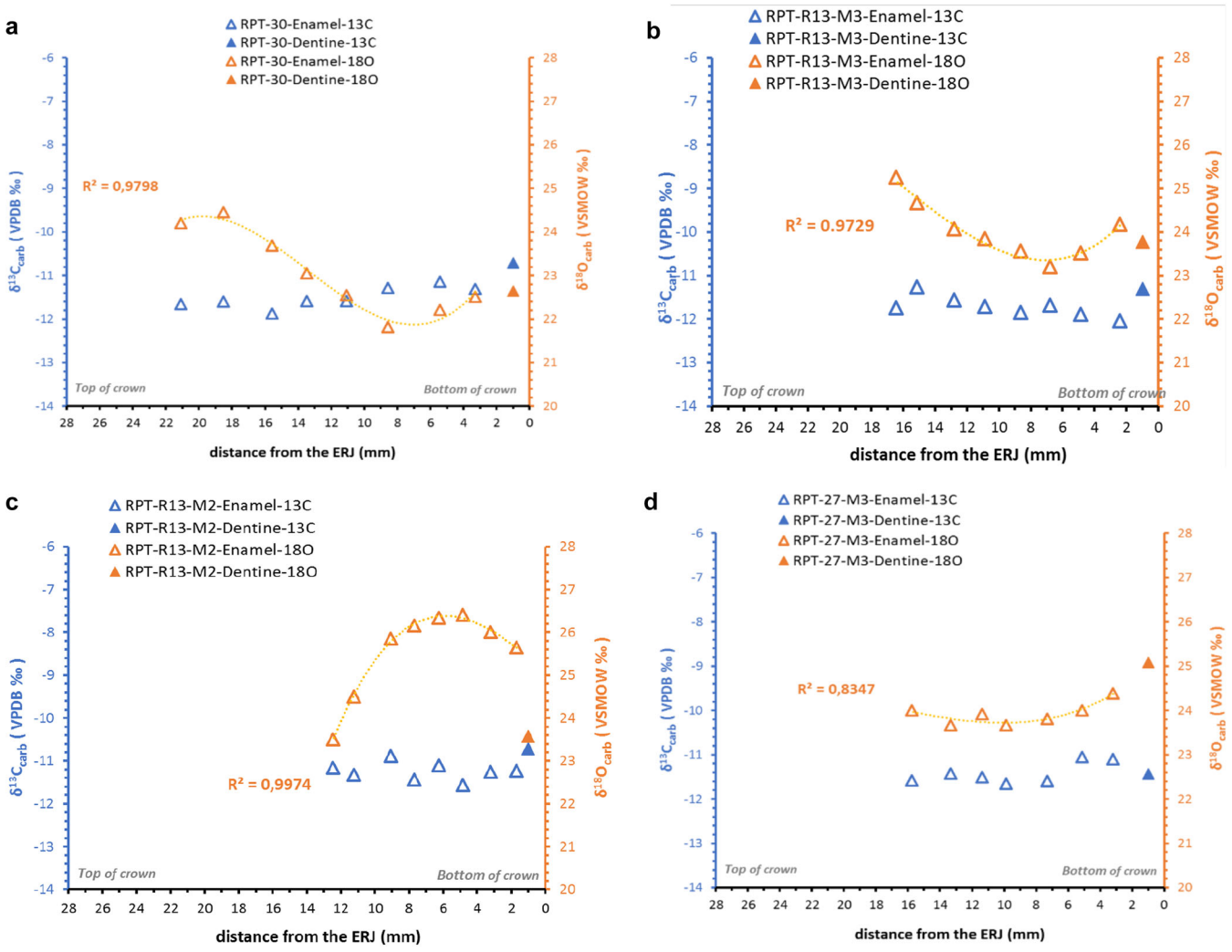

Figure 4. Incremental plots of red deer teeth showing $\delta^{18}O_{carb}$ curves: (a) annual cycle; (b) winter-only; (c) summer-only; and (d) flat profile.

© 2026 The Author(s). *Journal of Quaternary Science* Published by John Wiley & Sons Ltd.

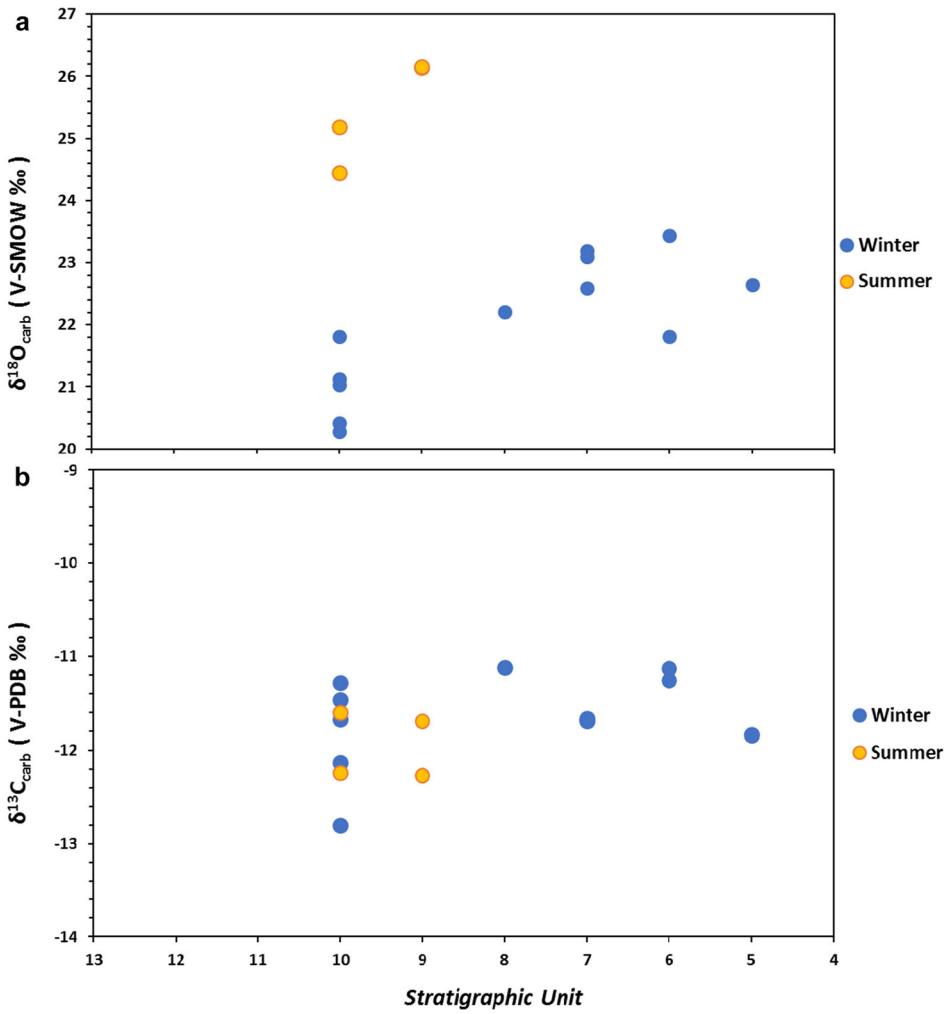

Figure 5. Isotopic values of red deer molars with well-defined seasonal profiles. (a) Maximum and minimum $\delta^{18}O_{carb}$ values along the crown length, used to estimate the mean monthly temperatures. (b) Corresponding $\delta^{13}C_{carb}$ values associated with the maximum and minimum $\delta^{18}O_{carb}$ values.

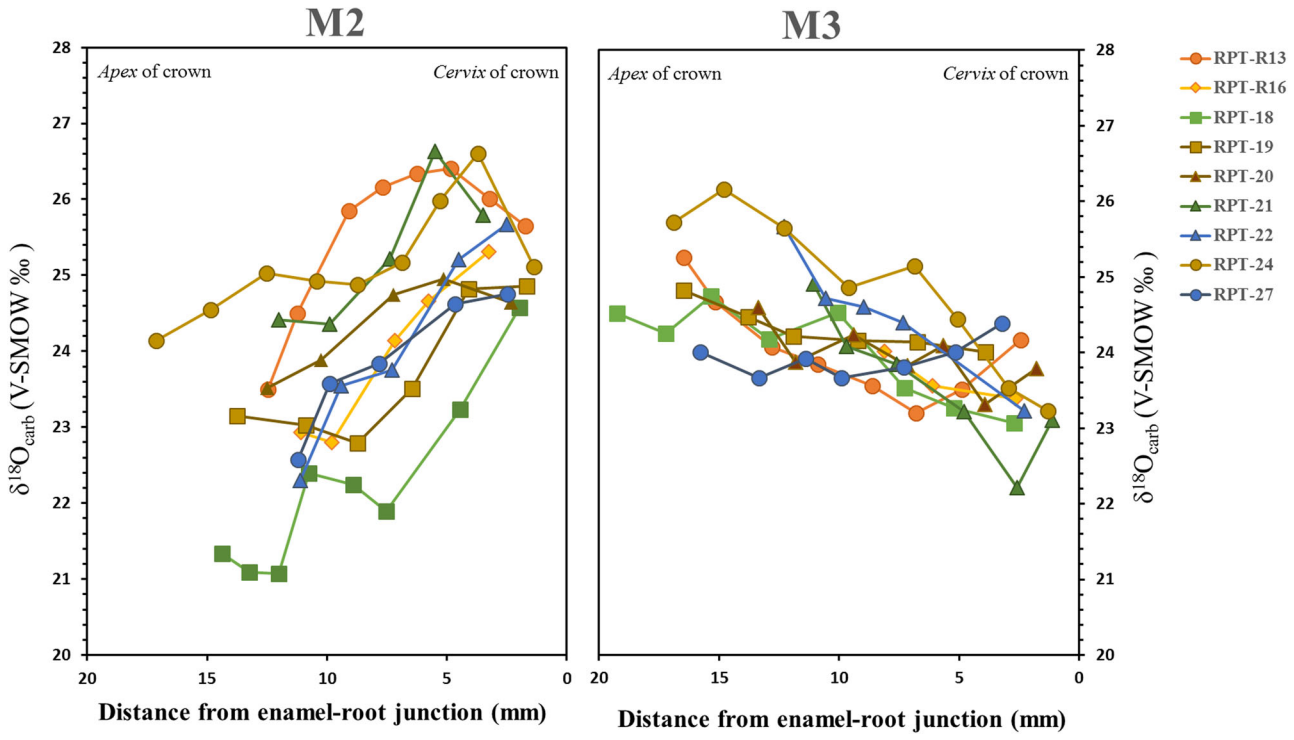

Figure 6. Incremental plots of intra-tooth oxygen isotope ratios ($\delta^{18}O_{carb}$) from second (M2) and third molars (M3) of 9 sampled red deer.

© 2026 The Author(s). *Journal of Quaternary Science* Published by John Wiley & Sons Ltd.

The highest intra-tooth variation in $\delta^{18}O_{carb}$ values (5.2‰) was observed in level 10, including all sub-layers (10a, b, c, and d), while the smallest intra-tooth variation was detected in layer 13, with a range of 3.2‰ (from to min: +20.9‰ to max: +24.1‰). Considering the archaeological layer 10a alone, it still yields the highest intra-tooth range of 4.8‰ among the entire stratigraphic series. In addition, the highest winter–summer contrasts were also observed in the teeth from layer 10 (a, b, c, and d), with a seasonal range of 4.9‰ (amplitude between the minimum point of winter and the maximum point of summer).

In addition to intra-tooth ranges, the intra-individual variation was also considered for individuals for which both second and third molars were collected ($n = 9$). Within an individual, the largest range in $\delta^{18}O_{carb}$ values is 4.4‰ (RPT-21, SU 9) and the lowest is 1.6‰ (RPT-20, SU 8). In the cumulative plotting of $\delta^{18}O_{carb}$ values, substantial differences in intra-individual (along M2 and M3) and some inter-individual variability can be detected (see Fig. 6). In general, lower or higher $\delta^{18}O_{carb}$ values are reached in the second molars in comparison with the corresponding third molars. Some overlap in the $\delta^{18}O_{carb}$ values can be observed between both molars, while the seasonal record of the third molars is postponed from one year compared with the second molar.

Reconstruction of the seasonal temperatures

To enable comparison between tooth enamel $\delta^{18}O_{carb}$ values and modeled precipitation $\delta^{18}O_w$ and air temperatures, the isotopic composition of drinking water consumed by red deer was first derived using Equation 3.2. The mean monthly air temperatures (MMTs) were then estimated using the European-scale transfer functions (Equations 3.3 and 3.4) for third molars showing clear seasonal isotopic patterns (Table 3). Samples lacking a clear seasonal signal, as well as second molars that may be influenced by maternal milk intake, were excluded from seasonal temperature reconstruction.

Based on the European-scale MMT estimates, cold winter conditions at Riparo Tagliente are recorded in stratigraphic level 10 (Fig. 7). The lowest reconstructed winter temperatures occur in layers 10a (−2.8°C) and 10b (−3.1°C), coinciding with the lowest $\delta^{13}C_{carb}$ and $\delta^{18}O_{carb}$ values. In contrast, a marked increase in summer temperatures is observed in stratigraphic layer 9, where the highest reconstructed summer MMT reaches 16.3°C. A secondary summer phase is also indicated in layer 10, with a summer MMT of 14.4°C.

Overall, the European-scale reconstruction consistently records colder winter conditions in stratigraphic level 10 and warmer summer conditions in level 9, indicating coherent seasonal temperature patterns across the studied stratigraphic sequence.

Discussion

Environmental conditions and red deer diet in the southern Alps during the Late Glacial (GS-2.1a to GI-1)

All the $\delta^{13}C_{carb}$ values (–13.3‰ to –10.7‰) obtained from the analyzed red deer enamel confirm the absence of a dense forest ecosystem in the region and are consistent with the presence of open canopy woodland during the Late Glacial period (e.g., Drucker et al., 2024; Fernández-García et al., 2024). Using a diet-bioapatite ^{13}C-trophic discrimination factor of +13.6‰ (see Drucker et al., 2024) for the per tooth averaged $\delta^{13}C_{carb}$ values (–12.8‰ to –11.2‰) of this study, the $\delta^{13}C_{diet}$ could be estimated to be between –26.4‰ and –24.8‰, which is not consistent with a diet derived from closed canopy conditions but rather indicates a more open landscape including open woodland. These $\delta^{13}C_{diet}$ values indicate a diet based on C_3 vegetation, likely dominated by temperate or cool-season grasses and a variety of dicots, including trees, shrubs, and herbaceous plants (e.g., Cerling et al., 1997). Relatively high bone collagen $\delta^{13}C_{coll}$ values (−20.5‰ to −18.4‰) in herbivores (red deer, roe deer, ibex,

Table 3. Mean monthly temperatures (MMTs) at the European scale following Reiss et al. (2024).

		Age			$\delta^{13}C_{carb}$	$\delta^{18}O_{carb}$	$\delta^{18}O_W$	MMT (°C) Europe	
Lab ID	Tooth	SU	Cal BP (IntCal20)	Stage	(‰, VPDB)	(‰, VSMOW)	(‰, VSMOW)	Winter	Summer
RPT-R6	M3 L	5	-	Older Dryas (GI-1c2)[1]	−11.8	22.6	−11.0	1.4	
RPT-R8	M3 R	6	-	Older Dryas (GI-1c2)[1]	−11.3	21.8	−11.8	-0.2	
RPT-R10	M3 L	6	-	Older Dryas (GI-1c2)[1]	−11.1	23.4	−10.2	2.9	
RPT-R11	M3 R	7b	-	Older Dryas (GI-1c2)[1]	−11.7	23.1	−10.6	2.2	
RPT-R13	M3 R	7	-	-	−11.7	23.2	−10.5	2.4	
RPT-R15	M3 R	7	-	-	−11.7	22.6	−11.1	1.3	
RPT-17	M3 R	8	14 809–13 505	Bølling–Allerød (GI-1)[2]	−11.1	22.2	−11.4	0.6	
RPT-23	M3 R	9	14 809–13 505	Bølling–Allerød (GI-1)[2]	−11.7	26.1	−7.5		16.3
RPT-24	M3 R	9	14 809–13 505	Bølling–Allerød (GI-1)[2]	−12.3	26.2	−7.5		16.3
RPT-26	M3 R	10a	15 553–14 294	Oldest Dryas (GS-2.1a), Bølling–Allerød (GI-1)[2]	−12.2	25.2	−8.5		14.4
RPT-36	M3 R	10a	15 553–14 294	Oldest Dryas (GS-2.1a), Bølling–Allerød (GI-1)[2]	−11.5	21.1	−12.5	−1.5	
RPT-37	M3 R	10a	15 553–14 294	Oldest Dryas (GS-2.1a), Bølling–Allerød (GI-1)[2]	−11.7	20.4	−13.2	−2.8	
RPT-29	M3 R	10b	-	-	−12.8	20.3	−13.4	−3.1	
RPT-30	M3 R	10c	16 175– 15 185	Oldest Dryas (GS-2.1a)[2]	−11.6	24.4	−9.2		12.9
					−11.3	21.8	−11.8	−0.2	
RPT-32	M3 R	10d	-	-	−12.1	21.0	−12.6	−1.7	

Abbreviations: L, left side; R, right side; SU, stratigraphic unit; (–), not determined yet; $\delta^{18}O_{W,}$ meteoric water oxygen isotope values converted from enamel $\delta^{18}O_{carb}$.

[1] Berto et al., 2018.

[2] Rasmussen et al., 2014.

© 2026 The Author(s). *Journal of Quaternary Science* Published by John Wiley & Sons Ltd.

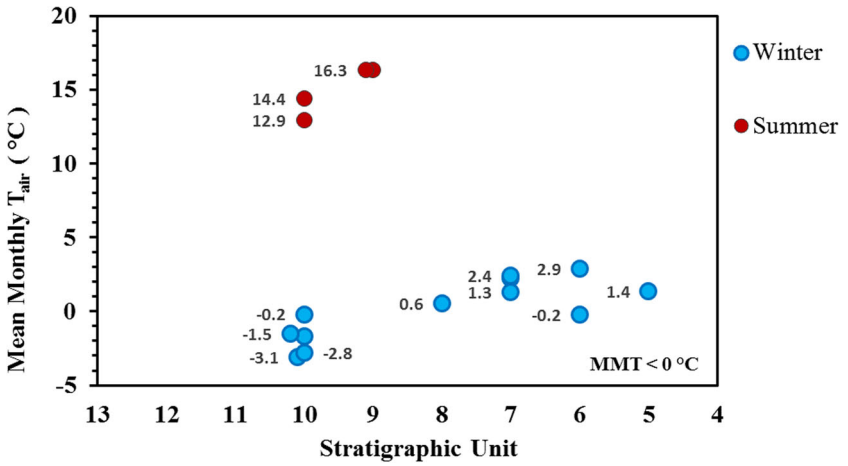

Figure 7. Reconstructed mean monthly air temperatures (°C) for the archaeological sequence at Riparo Tagliente, calculated using European-scale isotope–temperature transfer equations following Reiss et al. (2024).

chamois, and bovid) have previously been detected at the Tagliente rockshelter, being therefore consistent with the consumption of open-area C_3 plants ($\delta^{13}C_{diet} = -25.5‰$ to $-23.4‰$) (Gazzoni et al., 2013).

The variability of $\delta^{13}C_{carb}$ values from all red deer molars reflects both the climatic factors and landscape changes. After the LGM, the region transitioned from steppe-tundra, dominated by grasses, to temperate deciduous forests (Ravazzi et al., 2007), which aligns with the $\delta^{13}C$ values of plants deduced from the herbivore isotopic signatures. The relatively high $\delta^{13}C_{carb}$ values from level 13, chronologically referred to GS-2.1a, are consistent with a landscape dominated by wooded grasslands (Bartolomei et al., 1982; Gazzoni et al., 2013) (Fig. A5). Starting from level 10, at the transition between GS-2.1a and the onset of the Bølling–Allerød Interstadial (GI-1), some decrease in $\delta^{13}C_{carb}$ values is observed. This trend likely reflects an expansion of forest cover and a corresponding increase in red deer browsing behavior. In contrast, layers 6 and 5 show slightly higher $\delta^{13}C_{carb}$ values, possibly indicating a shift toward more open vegetation. An environmental fluctuation is also evident in the large mammal record in layers 7b-5, where open-habitat species like *C. ibex* and *A. alces* increase in frequency (Bartolomei et al., 1982; Rocci Ris 2006; Berto et al., 2018).

The results of this study are further supported by other intra-site proxies. Pollen analyses from the Epigravettian series at Riparo Tagliente suggest woodland expansion starting from layer 14, dominated by conifers (*Pinus sylvestris-mugo*) with the presence of some deciduous trees (e.g., *Quercus sp.*, *Tilia sp.*, *Corylus*). This assemblage suggests milder conditions during the Late Glacial Interstadial and is consistent with a heterogeneous, mosaic landscape combining open environments with patchy woodland cover (Bartolomei et al., 1982). Macro-mammal data show open-environment species in lower layers (17–14) and an increase of temperate species in the upper layers (12–5) (Rocci Ris, 2006; Fontana et al., 2009). The micro-mammal assemblage in layers 14–12 is dominated by fossorial taxa (e.g., *M. arvalis*), reflecting a mostly open landscape with limited forest. From level 11 onward, a decline in *M. arvalis* in the assemblage suggests gradual woodland expansion (Berto, 2013; Berto et al., 2018). Together, these proxies provide a coherent picture of progressive environmental change at Riparo Tagliente, highlighting a shift from open, periglacial habitats to more temperate, wooded environments in response to the Late Glacial climatic fluctuations.

At the individual level, evidence for seasonal dietary shifts was found in intra-tooth $\delta^{13}C_{carb}$ patterns. Slight $\delta^{13}C_{carb}$ increases during winter are observed in some specimens [e.g., RPT-R7 (SU 5), RPT-R8 (SU 6), RPT-30 (SU 10c), and RPT-35 (SU 13)], possibly reflecting increased intake of grasses, bushes, or xerophytes. Conversely, multiple specimens from all layers, except level 13, revealed a slight decrease in $\delta^{13}C_{carb}$ values in summer (e.g., RPT-18-M3, RPT-23M3, and RPT-27-M2), likely due to higher consumption of woody plants such as ^{13}C-depleted shrubs and deciduous trees (Drucker & Célérier, 2001; Ferrio et al., 2003; Drucker et al., 2011; Drucker et al., 2024). These seasonal dietary variations may suggest that red deer, as species inhabiting sparse forests in plains and valleys, could exploit multiple ecosystems at different altitudes (e.g., Gazzoni et al., 2013), varying in $\delta^{13}C$ plant compositions (Körner et al., 1988; Tieszen, 1991).

Similar results were reported in different studies on a regional and transregional scale. The bone collagen isotopic analysis for ibex and red deer species from Dalmeri, late Epigravettian rockshelter on the Marcèsina Plateau (NE, Italy), at over 1200 m a.s.l, yielded results (–21.6‰ to –19.4‰) consistent with a C_3 herbivore diet and an open landscape and some patchy forest during Allerød (GI-1a-c3) (Manzella et al., 2024). Relatively high $\delta^{13}C_{carb}$ values in red deer (–11.3‰ to –6.0‰), with intra-tooth variations ranging from 0.2‰ to 1.8‰, have been observed at the Upper Palaeolithic Serinyà caves (NE Catalonia, Spain), where an open landscape was also inferred (Drucker et al., 2024). The most elevated $\delta^{13}C_{carb}$ values suggest that red deer were mixed feeders inhabiting more xeric environments, potentially incorporating physiologically stressed plants into their winter diet. Red deer from Serinyà show higher carbon isotope values than those found in this study (–13.3‰ to –10.6‰), indicating regionally distinct red deer foraging environments in the two regions during the Late Pleistocene.

Paleoclimate and seasonality in the southern Alps (GS-2.1a to GI-1) through red deer enamel $\delta^{18}O$

Red deer $\delta^{18}O_{carb}$ values revealed a record of the seasonal variations in more than half of the measured specimens, that is, mainly winter in third molars and summer in second molars. This supports the established principle that second molars of red deer mainly record summer, the first season in red deer life, and third molars mostly reveal the winter of the year after (e.g., Stevens et al., 2011; Drucker et al., 2024). Third molars are expected to reflect an entire one-year seasonal cycle recorded during enamel formation; however, the limited seasonal records of this study are probably due to the presence of fractures on the crowns of the teeth. It also could be due to the complex nature of enamel maturation that does not allow to obtain an uninterrupted period of the isotopic variation experienced by the animal (e.g., Balasse, 2002; Zazzo et al., 2005). In this concept, the

© 2026 The Author(s). *Journal of Quaternary Science* Published by John Wiley & Sons Ltd.

reconstructed mean monthly temperatures (MMTs) comprise no more than one or two (summer and/or winter) seasons recorded during the tooth formation and should be considered as temporally averaged, relative estimates reflecting limited periods of tooth mineralization.

The red deer samples from Serinyà caves (mostly from Magdalenian occupation) also showed similar trends in $\delta^{18}O_{carb}$, with patterns largely reflecting winter conditions in the third molars (Drucker et al., 2024). Despite representing the same species, red deer from Serinyà showed relatively higher $\delta^{18}O_{carb}$ values, ranging from +23.2‰ to +27.4‰, and intra-tooth variation between 0.9‰ and 2.1‰. In contrast, red deer from this study displayed lower $\delta^{18}O_{carb}$, from +21.2‰ to +26.6‰, but greater intra-tooth variability, ranging from 0.5‰ to 3.5‰. While both sites reflect seasonal environmental fluctuations, the specimens from Riparo Tagliente revealed more pronounced winter–summer isotopic contrasts, potentially indicating greater climatic seasonality, differences in local hydrology, or distinct mobility strategies compared to contemporaneous populations in northeastern Catalonia.

In this study, layer 10 can be considered a significant layer in the sequence; however, we missed two more preceding layers (11 and 12) due to a lack of adequate specimens. The red deer population experienced either cold or mild winters (MMT values range from −3.1°C to −0.2°C in winter) as well as temperate warm summers in this Macrounit 10 that might suggest the ending of periglacial conditions and the onset of climate improvement during this phase (e.g., Bartolomei et al., 1982; Rocci Ris, 2006; Berto et al., 2018). Moreover, micro-mammal studies also clearly confirmed the beginning of GI-1 during level 10 with a slightly increased temperature in the coldest month (Berto et al., 2018). A similar interpretation was also observed in the intra-site malacofauna analysis that testified to the progressive climate improvement along the Epigravettian series 12–10 with a dominant xero-thermophilous species (Bartolomei et al., 1982). The intra-site micro-mammal assemblage starting from the following levels 9–8 and 7–5 testified to an impact of the general milder climate warming registered during GI-1 (Björck et al., 1998; Rasmussen et al., 2014), to some extent confirming our seasonal estimates. Relatively much warmer seasonal contrast in $\delta^{18}O_{carb}$ values can be observed in levels 9 and 10a (Fig. 7). Again, a gradual decline of temperatures was recorded in layer 6 (winter minimum of −0.2°C), which might likely correspond to the onset of another colder stage such as GI-1d, but it remains uncertain, pending precise radiocarbon dating for these stratigraphic units. In addition, an increase in cold-adapted species (e.g., *C. ibex*), together with cold-tolerant, moisture-dependent species (e.g., *A. alces*), was recorded in levels 7b-5, consistent with environmental conditions associated with GI-1c2 (Berto et al., 2018), a brief cold sub-event of Bølling–Allerød. Equivalent reconstructed paleotemperatures were inferred on a regional scale too. Chironomid assemblages testified to the mean summer (July) temperature reaching values of 10.5°C to 10.8°C in Northern Italy prior to the rapid warming of the Late Glacial Interstadial at ca. 14 700 cal a BP and around 13.8°C–15.3°C during Bølling–Allerød warming (Heiri et al., 2007). Overall, all temperature reconstructions discussed here should be regarded as relative estimates reflecting general climatic trends and seasonal contrasts rather than precise absolute temperature values. Independent environmental proxies would be required to further constrain the respective influence of temperature, precipitation regime, and moisture source on the observed isotopic signals.

Implications of Red Deer isotope profiles for Epigravettian subsistence at Riparo Tagliente

Oxygen-isotope profiles from red deer molars at Riparo Tagliente provide valuable insights into environmental conditions and prey availability that shaped Late Epigravettian subsistence strategies. In some stratigraphic units, several individuals showed similar oxygen isotope patterns, with similar absolute values of $\delta^{18}O_{carb,}$ indicating that these animals experienced similar environmental and hydrological conditions during tooth mineralization (e.g., Stevens et al., 2011). This is illustrated by RPT-11 and RPT-13 from level 7, and RPT-36 and RPT-37 from level 10a, which display comparable winter $\delta^{18}O_{carb}$ values and intra-individual profiles (Fig. A.3-3–6). Likewise, both M3 and M2 molars of RPT-19 and RPT-20 from layer 8 represent similarity in oxygen patterns and $\delta^{18}O_{carb}$ absolute values (Fig. A.3-4). This consistency points to stable $\delta^{18}O$ values in local drinking water and limited climatic variability within respective stratigraphic units. While these findings do not conclusively establish the seasonal site use, the repeated occurrence of similar isotopic profiles suggests that red deer were predictably and seasonally available, supporting a flexible and adaptive subsistence strategy by hunter-gatherers. In contrast, differences in isotopic ranges of specimens from the other layers may reflect differences in habitat use or mobility (e.g., Stevens et al., 2011).

Four teeth (RPT-19, RPT-20, RPT-27, and RPT-35) provided flat $\delta^{18}O_{carb}$ profiles with elevated values, broadly resembling summer-season isotopic signatures (Fig. A.3-4, 6, and 7). Rather than reflecting a local seasonal signal, these flat profiles likely represent an ecological pattern, suggesting that red deer may have spent the winter months in milder/lowland environments with reduced seasonal variability, away from the rock-shelter area. This $\delta^{18}O_{carb}$ isotopic stability could result from either the altitudinal effect (e.g., Flaim et al., 2013; Kern et al., 2014) or regular ingestion of isotopically buffered freshwater during colder seasons. Considering the site's geographical context, both interpretations are plausible. However, the corresponding intra-tooth carbon values do not record the expected elevation-related enrichment in ^{13}C (e.g., Männel et al., 2007), making high-altitude grazing less likely. The stable $\delta^{18}O$ profiles may thus be a result of buffered environmental conditions, either linked to mobility or access to large freshwater bodies. This, in turn, suggests that hunter-gatherer groups at Riparo Tagliente may have adapted their hunting strategies not only to seasonality but also to landscape features that shaped red deer distribution.

Conclusions

This study presents the first high-resolution enamel stable isotope data set on red deer (*C. elaphus*) from the Late Epigravettian levels of Riparo Tagliente, offering new insights into paleoenvironmental conditions, seasonal climate variability, and human subsistence strategies in the southeastern Italian Alps during the Late Glacial (GS-2.1a to GI-1).

Carbon isotope values ($\delta^{13}C_{carb}$) from red deer molars reflect a consistent diet based on C_3 vegetation and indicate that the landscape surrounding the site was dominated by open woodland environments. The absence of strongly negative $\delta^{13}C$ values confirms limited forest cover density throughout the sequence. Fluctuations in $\delta^{13}C_{carb}$ across stratigraphic layers align with regional vegetation shifts: slightly higher values in layers 13 and 5–6 suggest grassland dominance during colder periods, while slightly lower values in layers 10–8 may reflect forest expansion during the Bølling–Allerød Interstadial. Intra-tooth $\delta^{13}C$ variability also reveals seasonal shifts in diet, with some individuals consuming more grasses or shrubs in winter and woody browse in summer, supporting the interpretation that red deer exploited diverse habitats across different altitudes and microenvironments.

© 2026 The Author(s). *Journal of Quaternary Science* Published by John Wiley & Sons Ltd.

Oxygen isotope data ($\delta^{18}O_{carb}$) show clear seasonal trends in many individuals, with second molars typically reflecting summer and third molars recording winter conditions. This is consistent with the following principle: the second molars of red deer mainly record summer, the first season in red deer life, and third molars mostly reveal the winter of the year after based on the time range of enamel growth (Brown & Chapman, 1991b), and an isotopic study on modern red deer (Stevens et al., 2011). Estimated mean monthly temperatures (MMTs) derived from $\delta^{18}O_{carb}$ values suggest substantial climate variability across the sequence. The coldest winter temperatures were recorded in layers 10a and 10b (down to −3.1°C), while warmer summer conditions (up to 16.3°C) appeared in layer 9. These estimates are broadly consistent with independent regional paleoclimate reconstructions and point to fluctuating seasonal conditions during the Late Glacial, without implying a uniform or continuous climatic trend. Altogether, the isotopic evidence highlights the resilience and adaptability of Late Epigravettian hunter-gatherers in the Valpantena valley. The repeated availability of red deer across seasons, even in colder phases, supports the idea of stable open environments and the strategic use of ecotonal and freshwater-rich landscapes. These findings contribute to a more detailed reconstruction of Late Glacial environmental conditions in northern Italy and underscore the value of enamel carbonate isotopes in understanding faunal ecology and human subsistence at fine temporal and spatial scales. Future work should expand isotopic analyses to additional layers and taxa to obtain a more comprehensive picture of Late Glacial environmental dynamics. Further integration with zooarchaeological and mobility studies is also recommended to better understand red deer behavior and its implications for human subsistence strategies.

Acknowledgements. This study was conducted as part of the first author's MSc thesis within the Erasmus Mundus International Master in Quaternary and Prehistory (IMQP) program headed by the University of Ferrara (Italy) in collaboration with Muséum National d'Histoire Naturelle (France), Universitat Rovira i Virgili (Spain), Instituto Politecnico of Tomar (Portugal). Thanks are due to Prof. Hervé Bocherens and the Biogeology laboratory team (Valentina García-Huidobro, Magdalena Krajcarz, Maciej Krajcarz, Chris Baumann, Emily Milton, Freya Riedel, and Peter Tung) at the University of Tübingen for technical support during isotope analysis, and the faculties at Instituto Politécnico de Tomar and Università degli Studi di Ferrara for their academic guidance. The project was realized in the framework of Prin Project 2022 "After the ice" of the Italian Ministry of Research (MUR) coordinated by F. Fontana and funded by *EU—Next Generation EU"* (project identifier: 20228B294N). Open Access funding enabled and organized by Projekt DEAL.

Data Availability Statement

The data that support the findings of this study are available in the supplementary material of this article.

Supporting information

Additional supporting information can be found in the online version of this article.

Figure A1. Isotope values versus carbonate content (CO_3) with all data.

Figure A2. Comparison of isotopic profiles before and after carbonate (CO_3) quality control.

Figure A3. Isotopic incremental plots of all analyzed red deer teeth.

Figure A4. The mean values and standard deviations of $\delta^{13}C_{carb}$ and $\delta^{18}O_{carb}$ for each sampled red deer teeth (third molars – 33 pcs, second molars – 9 pcs).

Figure A5. Mean carbon isotope values ($\delta^{13}C_{carb}$), based only on third molars (M3).

Table A1. Results of the carbonate isotopic analysis ($\delta^{13}C$, $\delta^{18}O$) for red deer (*Cervus elaphus*) teeth.

Table A2. Classification of $\delta^{18}O_{carb}$ profiles.

References

Azorit, C., Analla, M., Carrasco, R., Calvo, J. & Muñoz-Cobo, J. (2002) Teeth eruption pattern in red deer (*Cervus elaphus hispanicus*) in southern Spain. *Anales de Biología*, 24, 107–114.

Balasse, M. (2002) Reconstructing dietary and environmental history from enamel isotopic analysis: Time resolution of intra-tooth sequential sampling. *International Journal of Osteoarchaeology*, 12(3), 155–165. Available from: https://doi.org/10.1002/oa.601

Balasse, M., Ambrose, S.H., Smith, A.B. & Price, T.D. (2002) The seasonal mobility model for prehistoric herders in the south-western Cape of South Africa assessed by isotopic analysis of sheep tooth enamel. *Journal of Archaeological Science*, 29(9), 917–932. Available from: https://doi.org/10.1006/jasc.2001.0787

Balasse, M., Smith, A.B., Ambrose, S.H. & Leigh, S.R. (2003) Determining sheep birth seasonality by analysis of tooth enamel oxygen isotope ratios: The Late Stone Age site of Kasteelberg (South Africa). *Journal of Archaeological Science*, 30(2), 205–215. Available from: https://doi.org/10.1006/jasc.2002.0833

Bartolomei, G., Broglio, A., Cattani, L., Cremaschi, M., Guerreschi, A., Mantovani, E. et al. (1982) I depositi Wurmiani del Riparo Tagliente. *Annali dell'Università di Ferrara (N.S.) sez*, 15(III 4), 61–105.

Berto, C. (2013) *Distribuzione ed evoluzione delle associazioni a piccoli mammiferi della penisola italiana durante il Pleistocene superiore (PhD Thesis)*. Ferrara: Università degli Studi di Ferrara. p. 158

Berto, C., Luzi, E., Canini, G.M., Guerreschi, A. & Fontana, F. (2018) Climate and landscape in Italy during Late Epigravettian. The Late Glacial small mammal sequence of Riparo Tagliente (Stallavena di Grezzana, Verona, Italy). *Quaternary Science Reviews*, 184, 132–142. Available from: https://doi.org/10.1016/j.quascirev.2017.07.022

Bertola, S., Broglio, A., Cassoli, P., Cilli, C., Cusinato, A., Dalmeri, G. et al. (2007) L'Epigravettiano recente nell'area prealpina e alpina orientale. In: Martini, F. (Ed.) *L'Italia tra 15.000 e 10.000 anni fa. Cosmopolitismo e regionalità nel Tardoglaciale*, vol. 5. Millenni, Studi di Archeologia Preistorica, pp. 39–94.

Bertola, S., Fontana, F. & Visentin, D. (2018) Lithic raw material circulation and settlement dynamics in the Upper Palaeolithic of the Venetian Prealps (NE Italy). A key-role for palaeoclimatic and landscape changes across the LGM? In: Borgia, V. & Cristiani, E., Eds *Palaeolithic Italy. Advanced studies on early human adaptation in the Apennine Peninsula*. Leiden: Sidestone Press. pp. 219–246.

Bertolini, M., Cristiani, E., Modolo, M., Visentini, P. & Romandini, M. (2016) Late epigravettian and mesolithic foragers of the eastern Alpine region: Animal exploitation and ornamental strategies at Riparo Biarzo (Northern Italy). *Quaternary International*, 423, 73–91.

Bietti, A. (1990) The late Upper Paleolithic in Italy: An overview. *Journal of World Prehistory*, 4(1), 95–155. Available from: https://doi.org/10.1007/BF00974820

Björck, S., Walker, M.J.C., Cwynar, L.C., Johnsen, S., Knudsen, K.-L. & Lowe, J.J., INTIMATE Members (1998) An event stratigraphy for the Last Termination in the North Atlantic region based on the Greenland ice-core record: A proposal by the INTIMATE group. *Journal of Quaternary Science*, 13(4), 283–292. Available from: https://doi.org/10.1002/(SICI)1099-1417(199807/08)13:4<283::AID-JQS386>3.0.CO;2-A

Bocherens, H. (2003) Isotopic biogeochemistry and the paleoecology of the mammoth steppe fauna. *Deinsea*, 9, 57–76.

Bocherens, H., Koch, P.L., Mariotti, A., Geraads, D. & Jaeger, J.-J. (1996) Isotopic biogeochemistry (^{13}C, ^{18}O) of mammalian enamel from African Pleistocene hominid sites. *Palaios*, 11(4), 306–318. Available from: https://doi.org/10.2307/3515241

Bortolini, E., Pagani, L., Oxilia, G., Posth, C., Fontana, F., Badino, F., et al. (2021) Early Alpine occupation backdates westward human migration in Late Glacial Europe. *Current Biology*, 31(11), 2484–2493. https://doi.org/10.1016/j.cub.2021.03.078

Bronk Ramsey, C., 2021. OxCal v.4.4.4 [software]. URL. https://c14.arch.ox.ac.uk/oxcal.html.

© 2026 The Author(s). *Journal of Quaternary Science* Published by John Wiley & Sons Ltd.

Brown, W.A.B. & Chapman, N.G. (1991a) The dentition of red deer (*Cervus elaphus*): A scoring scheme to assess age from wear of the permanent molariform teeth. *Journal of Zoology*, 224, 519–536.

Brown, W.A.B. & Chapman, N.G. (1991b) Age assessment of red deer (*Cervus elaphus*): From a scoring scheme based on radiographs of developing permanent molariform teeth. *Journal of Zoology*, 225(1), 85–97. Available from: https://doi.org/10.1111/j.1469-7998.1991.tb03803.x

Cavallo, G., Fontana, F., Gonzato, F., Guerreschi, A., Riccardi, M.P., Sardelli, G. et al. (2017) Sourcing and processing of ochre during the late upper Palaeolithic at Tagliente rock-shelter (NE Italy) based on conventional X-ray powder diffraction analysis. *Archaeological and Anthropological Sciences*, 9(5), 763–775. Available from: https://doi.org/10.1007/s12520-015-0299-3

Cerling, T.E., Harris, J.M., Ambrose, S.H., Leakey, M.G. & Solounias, N. (1997) Dietary and environmental reconstruction with stable isotope analyses of herbivore tooth enamel from the Miocene locality of Fort Ternan, Kenya. *Journal of Human Evolution*, 33(6), 635–650. Available from: https://doi.org/10.1006/jhev.1997.0151

Cilli, C., Giacobini, G., Guerreschi, A. & Gurioli, F. (2006) L'industria e gli oggetti ornamentali in materia dura animale dell'Epigravettiano di Riparo Tagliente, Verona, *Atti della XXXIX Riunione scientifica: Materie prime e scambi nella preistoria italiana: Nel cinquantenario della fondazione dell'Istituto italiano di preistoria e protostoria: Firenze, 25-27 novembre 2004: vol. I-II-III*. Florence: Istituto italiano di preistoria e protostoria. pp. 843–854.

Clutton-Brock, T.H., Guinness, F.E. & Albon, S.D. (1982) *Red deer: Behavior and ecology of two sexes*. Chicago: University of Chicago press

Coplen, T.B. (1988) Normalization of oxygen and hydrogen isotope data. *Chemical Geology: Isotope Geoscience section*, 72(4), 293–297. Available from: https://doi.org/10.1016/0168-9622(88)90042-5

Cusinato, A. & Bassetti, M. (2007) Popolamento umano e paleoambiente tra la culminazione dell'ultima glaciazione e l'inizio dell'Olocene in area trentina e zone limitrofe. *Studi Trentini di Scienze Naturali, Acta Geologica*, 82, 2005 43–63.

Drucker, D.G., Bridault, A., Cupillard, C., Hujic, A. & Bocherens, H. (2011) Evolution of habitat and environment of red deer (*Cervus elaphus*) during the Late-glacial and early Holocene in eastern France (French Jura and the western Alps) using multi-isotope analysis ($\delta^{13}C$, $\delta^{15}N$, $\delta^{18}O$, $\delta^{34}S$) of archaeological remains. *Quaternary International*, 245, 268–278. Available from: https://doi.org/10.1016/j.quaint.2011.07.019

Drucker, D. & Célérier, G. (2001) Teneurs en carbone-13 du collagène de grands mammifères du site de Pont d'Ambon (Dordogne, France): Implications pour l'environnement et son exploitation au Tardiglaciaire dans le Sud-ouest de la France. PALEO. *Revue d'archéologie préhistorique*, 13, 145–158. https://doi.org/10.4000/paleo.1024

Drucker, D.G., Rivals, F., Nadal, J., Rufí, I., Soler, J., Soler, N. et al. (2024) Ecology of large ungulates in the northeastern Iberian Peninsula during the Upper Palaeolithic through stable isotopes and tooth wear analysis. *Quaternary Environments and Humans*, 2(4)100011. Available from: https://doi.org/10.1016/j.qeh.2024.100011.

Fasser, N., Visentin, D., Duches, R., Peresani, M. & Fontana, F. (2024) Lithic projectile technology in the western Late Epigravettian: The case study of north-eastern Italy. *Quaternary International*, 694, 70–90.

Fasser, N., Visentin, D. & Fontana, F. (2022) Characterising Late Palaeolithic manufacturing traditions: Backed points production methods in the Late Epigravettian sequence of Riparo Tagliente (NE Italy). *Journal of Archaeological Science: Reports*, 42, 103343.

Fernández-García, M., Pederzani, S., Britton, K., Agudo-Pérez, L., Cicero, A., Geiling, J.M. et al. (2024) Palaeoecology of ungulates in northern Iberia during the Late Pleistocene through isotopic analysis of teeth. *Biogeosciences*, 21(19), 4413–4437. Available from: https://doi.org/10.5194/bg-21-4413-2024

Ferrio, J.P., Voltas, J. & Araus, J.L. (2003) Use of carbon isotope composition in monitoring environmental changes. *Management of Environmental Quality: An International Journal*, 14(1), 82–98. Available from: https://doi.org/10.1108/14777830310460405

Filippi, M.L., Heiri, O., Arpenti, E., Angeli, N., Bortolotti, M., Lotter, A. et al. (2007) Evoluzione paleoambientale dal Tardoglaciale a oggi ricostruita attraverso lo studio dei sedimenti del Lago di Lavarone (Altopiano di Folgaria e Lavarone, Trentino). *Studi Trentini di Scienze Naturali Acta Geologica*, 279–298.

Flaim, G., Camin, F., Tonon, A. & Obertegger, U. (2013) Stable isotopes of lakes and precipitation along an altitudinal gradient in the Eastern Alps. *Biogeochemistry*, 116(1), 187–198. Available from: https://doi.org/10.1007/s10533-013-9855-z

Fontana, F., Cilli, C., Cremona, M.G., Giacomo, G., Fabio, G., Jeremie, L. et al. (2009) Recent data on the Late Epigravettian occupation at Riparo Tagliente, Monti Lessini (Grezzana, Verona): a multidisciplinary perspective. *Preistoria Alpina*, 44, 51–60.

Fontana, F., Falceri, L., Gajardo, A., Bertola, S., Cremona, M.G., Cavulli, F. et al. (2018) Re-colonising the Southern Alpine fringe. Diachronic data on the use of sheltered space in the Late Epigravettian site of Riparo Tagliente, In *Palaeolithic Italy. Advanced studies on early human adaptations in the Apennine peninsula*. Verona, Italy: Sidestone Press. pp. 287–310.

Fontana, F., Guerreschi, A., Bertola, S., Cremona, M.G., Cavulli, F., Falceri, L. et al. (2015) *I livelli più antichi della serie epigravettiana "interna" di Riparo Tagliente: sfruttamento delle risorse litiche e sistemi tecnici* (Vol. XXVIII). Studi di Preistoria e Protostoria 2. pp. 43–52.

Frisia, S., Borsato, A., Spötl, C., Villa, I.M. & Cucchi, F. (2005) Climate variability in the SE Alps of Italy over the past 17 000 years reconstructed from a stalagmite record. *Boreas*, 34, 445–455. Available from: https://doi.org/10.1080/03009480500231336

Gazzoni, V., Goude, G., Herrscher, E., Guerreschi, A., Antonioli, F. & Fontana, F. (2013) Late Upper Palaeolithic human diet: First stable isotope evidence from Riparo Tagliente (Verona, Italy). *Bulletins et mémoires de la Société d'anthropologie de Paris*, 25, 103–117. Available from: https://doi.org/10.1007/s13219-012-0079-x

Godawa, J. (1989). Age determination in the red deer (*Cervus elaphus*). *Acta Theriologica*, 34(28), 381–384.

Heiri, O., Filippi, M.L. & Lotter, A.F. (2007) Lateglacial summer temperature in the Trentino area (Northern Italy) as reconstructed by fossil chironomid assemblages in Lago di Lavarone (1100 m a.s.l.). *Studi Trentini di Scienze Naturali: Acta Geologica*, 82, 299–308.

Heptner, V.G., Nasimovich, A.A. & Bannikov, A.G. (1989). *Mammals of the Soviet Union* (Vol. 1: Ungulates). New York, USA: E.J. Brill.

Iacumin, P., Bocherens, H., Mariotti, A. & Longinelli, A. (1996) Oxygen isotope analyses of co-existing carbonate and phosphate in biogenic apatite: A way to monitor diagenetic alteration of bone phosphate. *Earth and Planetary Science Letters*, 142(1), 1–6. Available from: https://doi.org/10.1016/0012-821X(96)00093-3

Ivy-Ochs, S., Kerschner, H., Reuther, A., Preusser, F., Heine, K., Maisch, M. et al. (2008) Chronology of the last glacial cycle in the European Alps. *Journal of Quaternary Science*, 23(6–7), 559–573.

Kern, Z., Kohán, B. & Leuenberger, M. (2014) Precipitation isoscape of high reliefs: Interpolation scheme designed and tested for monthly resolved precipitation oxygen isotope records of an Alpine domain. *Atmospheric Chemistry and Physics*, 14(4), 1897–1907. Available from: https://doi.org/10.5194/acp-14-1897-2014

Koch, P.L. (2007) Isotopic Study of the Biology of Modern and Fossil Vertebrates. In: Michener, R. & Lajtha, K. (Eds.) *Stable Isotopes in Ecology and Environmental Science*, 2nd edition. Boston: Blackwell Publishing Ltd, pp. 99–154. Available from: https://doi.org/10.1002/9780470691854.ch5

Koch, P.L., Tuross, N. & Fogel, M.L. (1997) The effects of sample treatment and diagenesis on the isotopic integrity of carbonate in biogenic hydroxylapatite. *Journal of Archaeological Science*, 24, 417–429. Available from: https://doi.org/10.1006/jasc.1996.0126

Kohn, M. & Cerling, T. (2002) Stable Isotope Compositions of Biological Apatite. In: Kohn, M.J., Rakovan, J. & Hughes, J.M., Ed. *Reviews in mineralogy and geochemistry. Phosphates. Geochemical, Geobiological, and Materials Importance*, 48. Washington, D.C: Mineralogical Society of America. pp. 455–488, https://doi.org/10.2138/rmg.2002.48.12

Kohn, M.J., Schoeninger, M.J. & Valley, J.W. (1998) Variability in oxygen isotope compositions of herbivore teeth: Reflections of seasonality or developmental physiology? *Chemical Geology*, 152(1), 97–112. Available from: https://doi.org/10.1016/S0009-2541(98)00099-0

Körner, C., Farquhar, G.D. & Roksandic, Z. (1988) A global survey of carbon isotope discrimination in plants from high altitude.

© 2026 The Author(s). *Journal of Quaternary Science* Published by John Wiley & Sons Ltd.

Oecologia, 74(4), 623–632. Available from: https://doi.org/10.1007/BF00380063

Lambeck, K., Rouby, H., Purcell, A., Sun, Y. & Sambridge, M. (2014) Sea level and global ice volumes from the Last Glacial Maximum to the Holocene. *Proceedings of the National Academy of Sciences*, 111(43), 15296–15303. Available from: https://doi.org/10.1073/pnas.1411762111

Lee-Thorp, J. & Sponheimer, M. (2003) Three case studies used to reassess the reliability of fossil bone and enamel isotope signals for paleodietary studies. *Journal of Anthropological Archaeology*, 22(3), 208–216. Available from: https://doi.org/10.1016/S0278-4165(03)00035-7

Magny, M., Aalbersberg, G., Bégeot, C., Benoit-Ruffaldi, P., Bossuet, G., Disnar, J. et al. (2006) Environmental and climatic changes in the Jura mountains (eastern France) during the Lateglacial–Holocene transition: A multi-proxy record from Lake Lautrey. *Quaternary Science Reviews*, 25(5), 414–445. Available from: https://doi.org/10.1016/j.quascirev.2005.02.005

Magyari, E.K., Kuneš, P., Jakab, G., Sümegi, P., Pelánková, B., Schäbitz, F. et al. (2014) Late Pleniglacial vegetation in eastern-central Europe: Are there modern analogues in Siberia? *Quaternary Science Reviews*, 95, 60–79. Available from: https://doi.org/10.1016/j.quascirev.2014.04.020

Männel, T., Auerswald, K. & Schnyder, H. (2007) Altitudinal gradients of grassland carbon and nitrogen isotope composition are recorded in the hair of grazers. *Global Ecology and Biogeography*, 16, 583–592. Available from: https://doi.org/10.1111/j.1466-8238.2007.00322.x

Manzella, G., Fontana, A., Marín-Arroyo, A.B., Agudo Pérez, L., Peresani, M. & Duches, R. (2024) Paleoecology of mid-mountain Alps (Trentino, Italy) between Greenland interstadial 1 and Early Holocene. Carbon and nitrogen stable isotope analysis of ibex and red deer. *Quaternary Science Reviews*, 328. 108549. Available from: https://doi.org/10.1016/j.quascirev.2024.108549.

Medina, E., Montes, G., Cuevas, E. & Rokzandic, Z. (1986) Profiles of CO_2 concentration and $\delta^{13}C$ values in tropical rain forests of the upper Rio Negro Basin, Venezuela. *Journal of Tropical Ecology*, 2(3), 207–217. Available from: https://doi.org/10.1017/S0266467400000821

van der Merwe, N.J. & Medina, E. (1989) Photosynthesis and ratios in Amazonian rain forests. *Geochimica et Cosmochimica Acta*, 53(5), 1091–1094. Available from: https://doi.org/10.1016/0016-7037(89)90213-5

van der Merwe, N.J. & Medina, E. (1991) The canopy effect, carbon isotope ratios and foodwebs in amazonia. *Journal of Archaeological Science*, 18(3), 249–259. Available from: https://doi.org/10.1016/0305-4403(91)90064-V

Monegato, G., Ravazzi, C., Culiberg, M., Pini, R., Bavec, M., Calderoni, G. et al. (2015) Sedimentary evolution and persistence of open forests between the south-eastern Alpine fringe and the Northern Dinarides during the Last Glacial Maximum. *Palaeogeography, Palaeoclimatology, Palaeoecology*, 436, 23–40. Available from: https://doi.org/10.1016/j.palaeo.2015.06.025

Montoya, C., Duches, R., Fontana, F., Peresani, M. & Visentin, D. (2018) Peuplement tardiglaciaire et holocène ancien des Préalpes de la Vénétie (Italie Nord Orientale): éléments de confrontation. In: Averbouh, A., Bonnet-Jacquement, P. & Cleyet- Merle, J.J. (Eds.), *L'Aquitaine à la fin des temps glaciaires - Aquitaine at the end of the Ice Age. Les sociétés de la transition du Paléolithique final au début du Mésolithique dans l'espace Nord aquitain*. Actes de la table ronde organisée en hommage à Guy Célérier, Les Eyzie-de-Tayac, PALEO, numéro spécial. pp. 193–202.

Oxilia, G., Bortolini, E., Badino, F., Bernardini, F., Gazzoni, V., Lugli, F. et al. (2021) Exploring late Paleolithic and Mesolithic diet in the Eastern Alpine region of Italy through multiple proxies. *American Journal of Physical Anthropology*, 174(2), 232–253. Available from: https://doi.org/10.1002/ajpa.24128

Passey, B.H. & Cerling, T.E. (2002) Tooth enamel mineralization in ungulates: Implications for recovering a primary isotopic time-series. *Geochimica et Cosmochimica Acta*, 66, 3225–3234. Available from: https://doi.org/10.1016/S0016-7037(02)00933-X

Peresani, M., Monegato, G., Ravazzi, C., Bertola, S., Margaritora, D., Breda, M. et al. (2021) Hunter-gatherers across the great Adriatic-Po region during the Last Glacial Maximum: Environmental and cultural dynamics. *Quaternary International*, 581–582, 128–163. Available from: https://doi.org/10.1016/j.quaint.2020.10.007

Price, T.D., Meiggs, D., Weber, M.J. & Pike-Tay, A. (2017) The migration of Late Pleistocene reindeer: isotopic evidence from northern Europe. *Archaeological and Anthropological Sciences*, 9(3), 371–394. https://link.springer.com/article/10.1007/s12520-015-0290-z

Rasmussen, S.O., Bigler, M., Blockley, S.P., Blunier, T., Buchardt, S.L., Clausen, H.B. et al. (2014) A stratigraphic framework for abrupt climatic changes during the Last Glacial period based on three synchronized Greenland ice-core records: Refining and extending the INTIMATE event stratigraphy. *Quaternary Science Reviews*, 106, 14–28. Available from: https://doi.org/10.1016/j.quascirev.2014.09.007

Ravazzi, C., Peresani, M., Pini, R. & Vescovi, E. (2007) Il Tardoglaciale nelle Alpi italiane e in Pianura Padana. Evoluzione stratigrafica, storia della vegetazione e del popolamento antropico. *Il Quaternario*, 20, 163–184.

Reimer, P.J., Austin, W.E.N., Bard, E., Bayliss, A., Blackwell, P.G., Bronk Ramsey, C. et al. (2020) The IntCal20 northern hemisphere radiocarbon age calibration curve (0–55 cal kBP). *Radiocarbon*, 62(4), 725–757. Available from: https://doi.org/10.1017/RDC.2020.41

Reiss, L., Mayr, C., Pasda, K., Joachimski, M.M., Einwögerer, T., Händel, M. et al. (2024) Seasonal climate variations during Marine Isotope Stages 3 and 2 inferred from high-resolution oxygen isotope ratios in horse tooth enamel from Lower Austria. *Journal of Quaternary Science*, 39(4), 531–546. Available from: https://doi.org/10.1002/jqs.3613

Rocci Ris, A. (2006) I macromammiferi di Riparo Tagliente. Archeozoologia e tafonomia dei livelli epigravettiani (PhD Thesis), Torino: Università degli Studi di Torino, 535 p.

Ruiz-Redondo, A., Vukosavljević, N., Tomasso, A., Peresani, M., Davies, W. & Vander Linden, M. (2022) Mid and Late Upper Palaeolithic in the Adriatic Basin: Chronology, transitions and human adaptations to a changing landscape. *Quaternary Science Reviews*, 276. 107319. Available from: https://doi.org/10.1016/j.quascirev.2021.107319.

Stevens, R.E., Balasse, M. & O'Connell, T.C. (2011) Intra-tooth oxygen isotope variation in a known population of red deer: Implications for past climate and seasonality reconstructions. *Palaeogeography, Palaeoclimatology, Palaeoecology*, 301(1), 64–74. Available from: https://doi.org/10.1016/j.palaeo.2010.12.021

Tieszen, L.L. (1991) Natural variations in the carbon isotope values of plants: Implications for archaeology, ecology, and paleoecology. *Journal of Archaeological Science*, 18(3), 227–248. Available from: https://doi.org/10.1016/0305-4403(91)90063-U

Willis, K.J., Rudner, E. & Sümegi, P. (2000) The full-glacial forests of central and Southeastern Europe. *Quaternary Research*, 53(2), 203–213. Available from: https://doi.org/10.1006/qres.1999.2119

Wright, L.E. & Schwarcz, H.P. (1998) Stable carbon and oxygen isotopes in human tooth enamel: Identifying breastfeeding and weaning in prehistory. *American Journal of Physical Anthropology*, 106(1), 1–18. Available from: https://doi.org/10.1002/(sici)1096-8644(199805)106:1<1::aid-ajpa1>3.0.co;2-w

Wright, L.E. & Schwarcz, H.P. (1999) Correspondence between stable carbon, oxygen and nitrogen isotopes in human tooth enamel and dentine: Infant diets at Kaminaljuyú. *Journal of Archaeological Science*, 26(9), 1159–1170. Available from: https://doi.org/10.1006/jasc.1998.0351

Yavuz, O.E., Oxilia, G., Silvestrini, S., Tassoni, L., Reiter, E., Drucker, D.G. et al. (2024) Biomolecular analysis of the Epigravettian human remains from Riparo Tagliente in northern Italy. *Communications Biology*, 7, 1415. Available from: https://doi.org/10.1038/s42003-024-06979-9

Zazzo, A., Balasse, M. & Patterson, W.P. (2005) High-resolution $\delta^{13}C$ intratooth profiles in bovine enamel: Implications for mineralization pattern and isotopic attenuation. *Geochimica et Cosmochimica Acta*, 69(14), 3631–3642. Available from: https://doi.org/10.1016/j.gca.2005.02.031

Zorzi, F. & Mezzana, F. (1962) Provincia di Verona. *Grezzana. Rivista di Scienze Preistoriche*, 17, 284–285.

© 2026 The Author(s). *Journal of Quaternary Science* Published by John Wiley & Sons Ltd.